

Supplementary Materials

Synthesis and characterization of new triazole-bispidinone scaffolds and their metal complexes for catalytic applications

Arianna Rossetti,^{1,2,*} Alessandro Sacchetti,^{1,2} Fiorella Meneghetti,^{3,*} Greta Colombo Dugoni,¹ Matteo Mori,³ Carlo Castellano⁴

¹ Department of Chemistry, Materials and Chemical Engineering “G. Natta”, Politecnico di Milano, via Mancinelli 7, 20131 Milano, Italy

² INSTM - Local Unit c/o Politecnico di Milano, via Mancinelli 7, 20131 Milano, Italy

³ Department of Pharmaceutical Sciences, University of Milan, via L. Mangiagalli 25, 20133 Milano, Italy

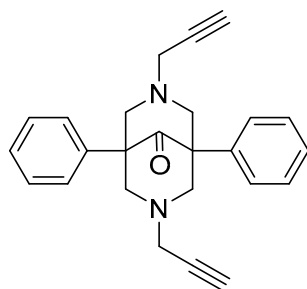
⁴ Department of Chemistry, University of Milan, via C. Golgi 19, 20133 Milano, Italy

* Correspondence: arianna.rossetti@polimi.it; fiorella.meneghetti@unimi.it

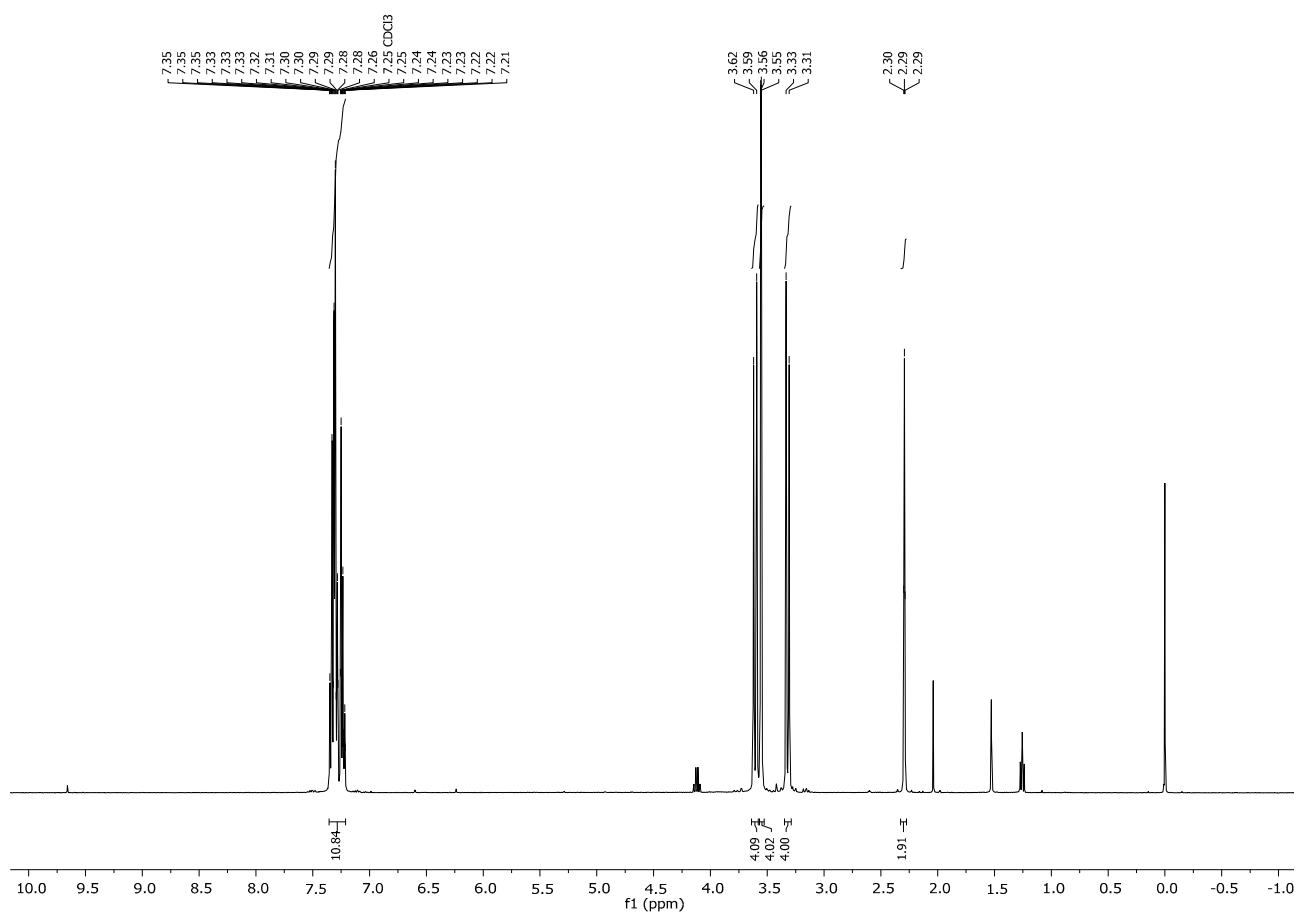
Table of Contents

1. NMR DATA	Pag. S3
2. NMR TITRATION OF BISPIDINE-METAL COMPLEXES	Pag. S41
3. ESI-MS ANALYSES	Pag. S44

1. NMR DATA



1



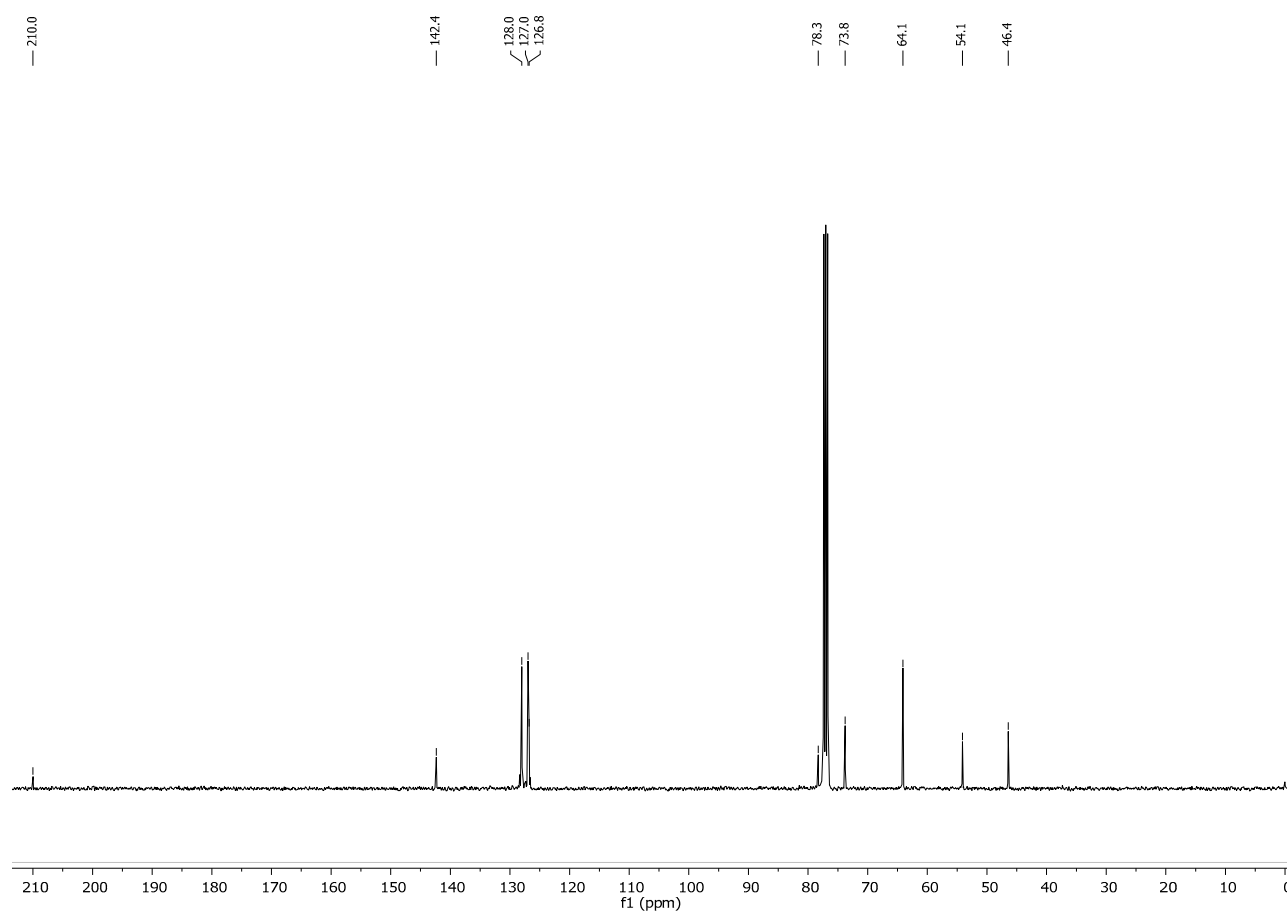
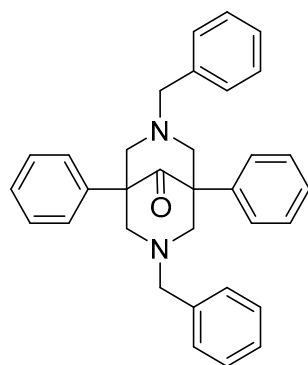


Figure S1. ^1H and ^{13}C -NMR spectra of compound **1**.



2

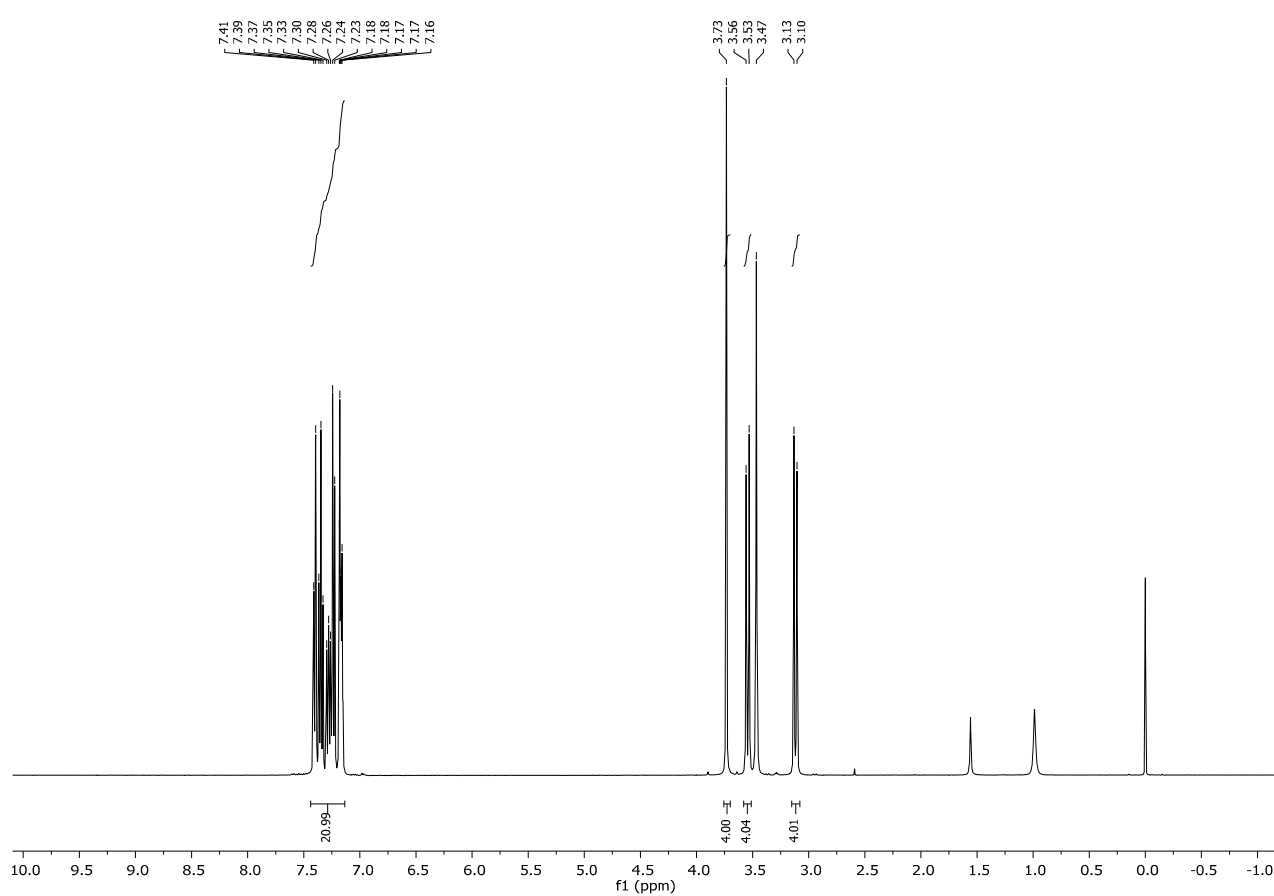


Figure S2. ^1H -NMR spectrum of compound **2** in accordance with literature. [Black, D.S.C.; Deacon, G.B.; Rose, M. Synthesis and metal complexes of symmetrically N-substituted bispidinones. *Tetrahedron* **1995**, *51*, 2055–2076, doi:10.1016/0040-4020(94)01069-C.]

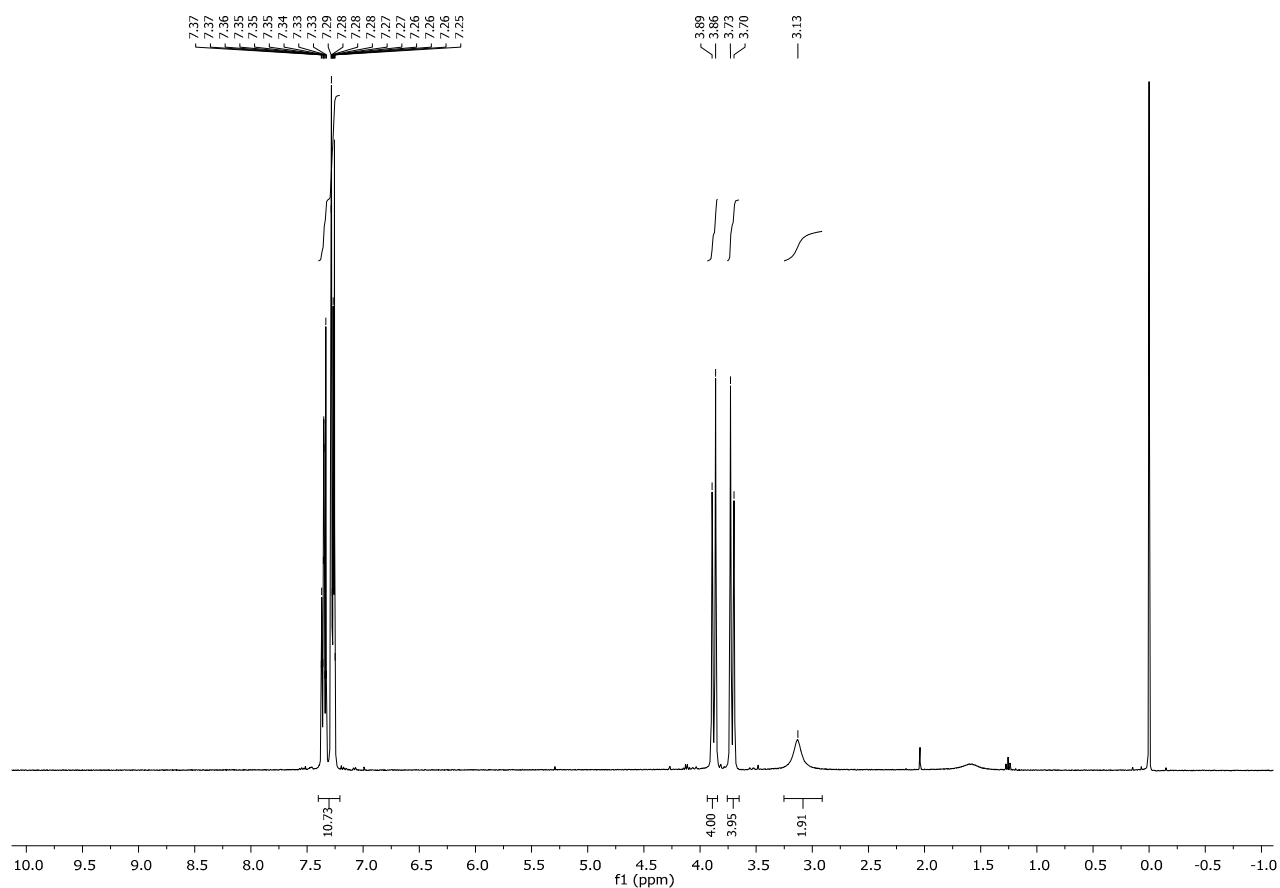
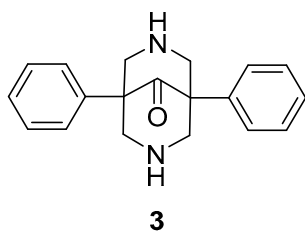
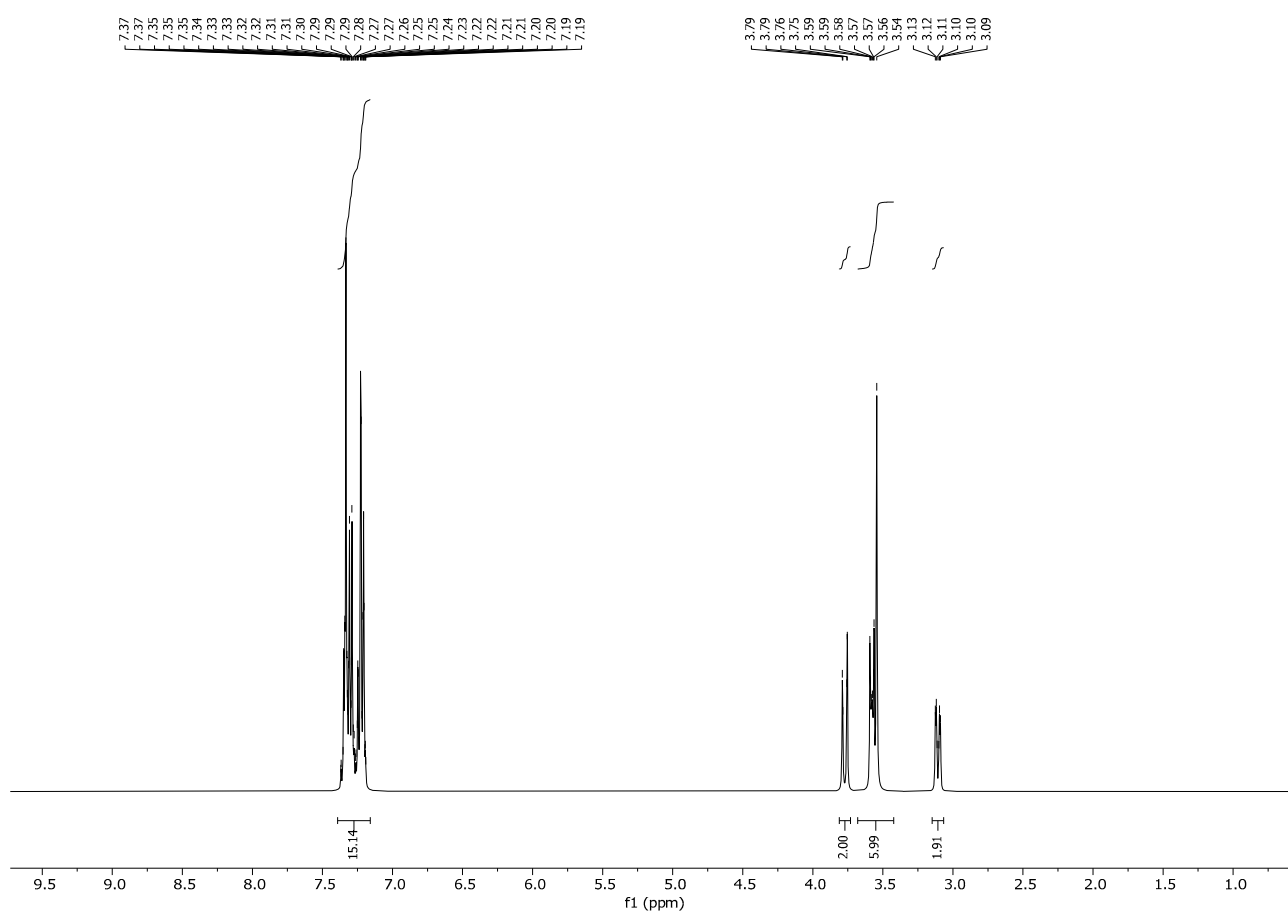
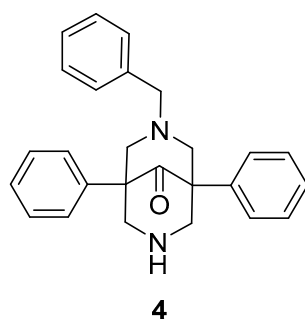


Figure S3. ^1H -NMR spectrum of compound **3** in accordance with literature. [Black, D.S.C.; Deacon, G.B.; Rose, M. Synthesis and metal complexes of symmetrically N-substituted bispidinones. *Tetrahedron* **1995**, 51, 2055–2076, doi:10.1016/0040-4020(94)01069-C.]



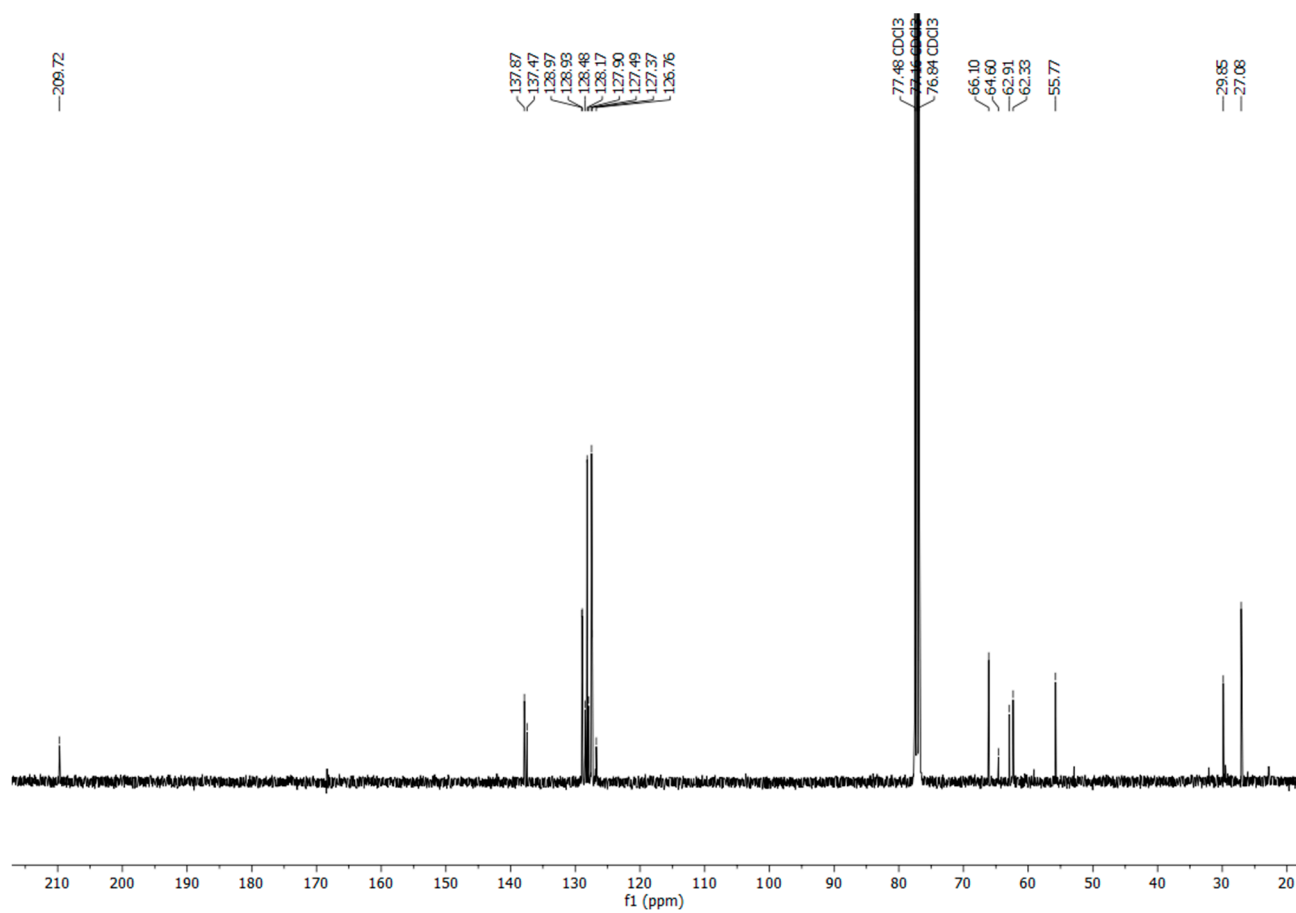
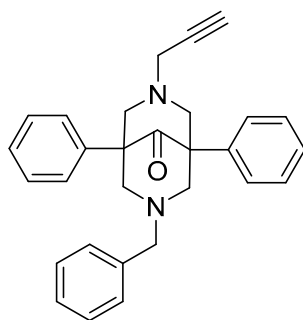
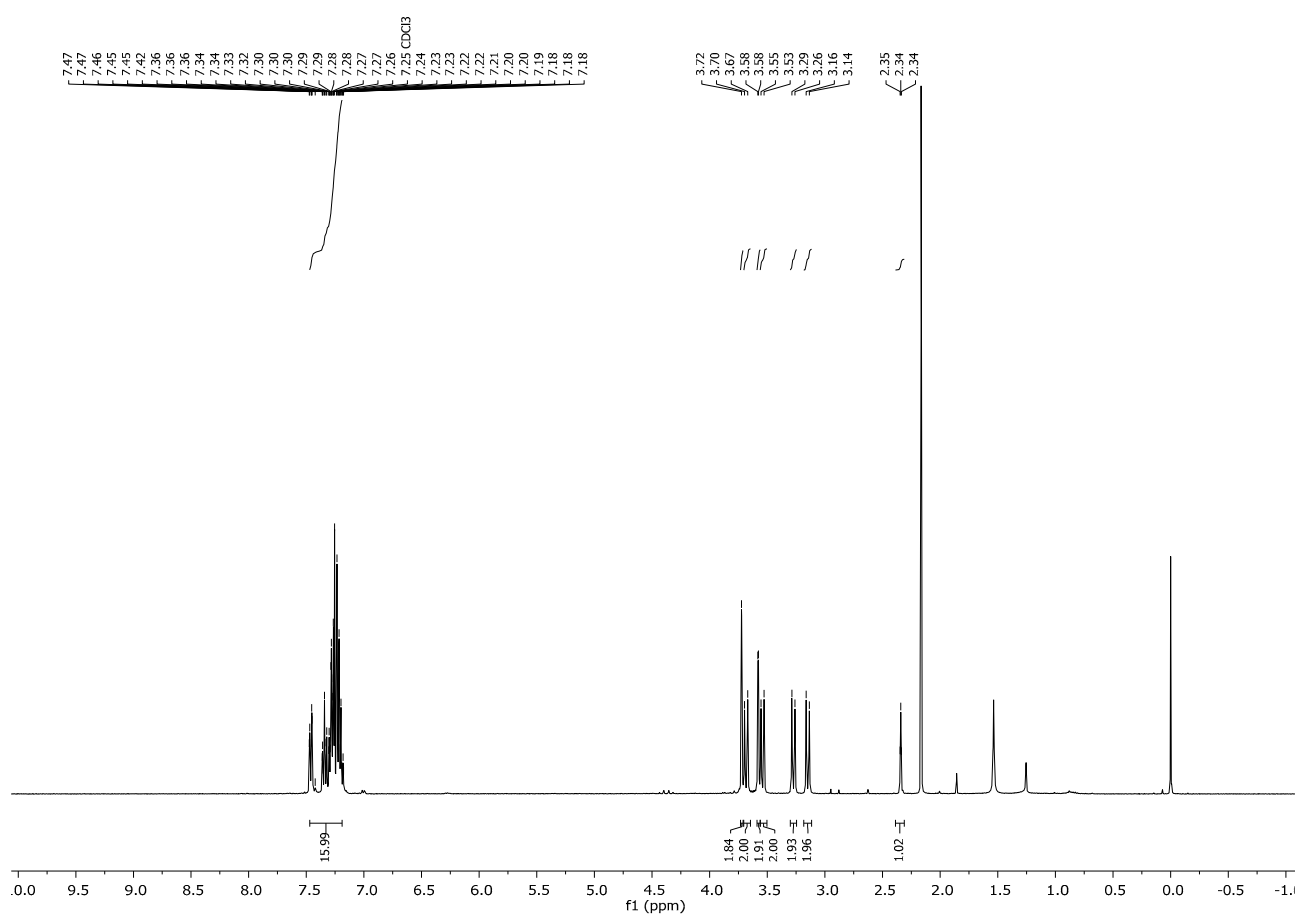


Figure S4. ^1H and ^{13}C -NMR spectra of compound 4.



5



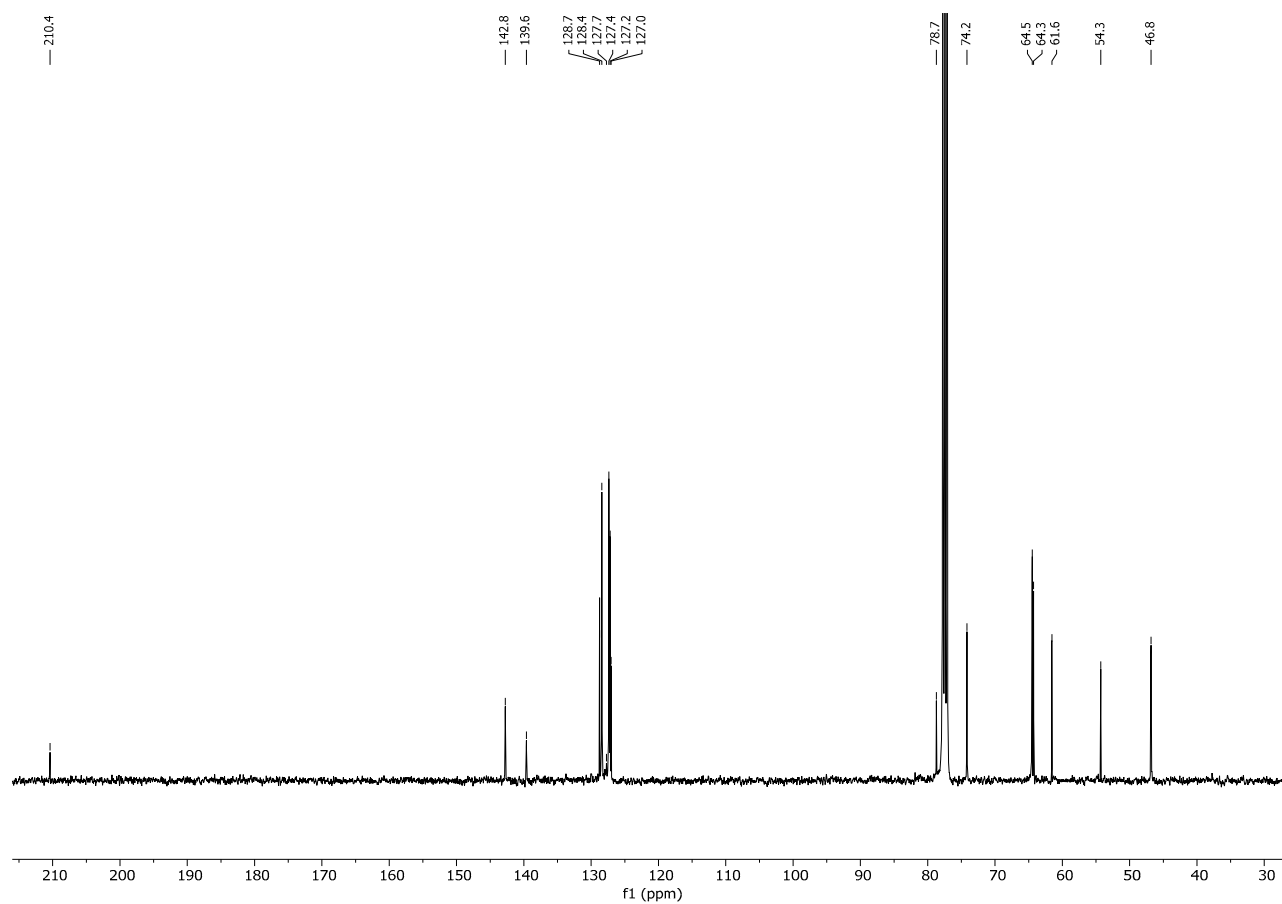


Figure S5. ^1H and ^{13}C -NMR spectra of compound **5**.

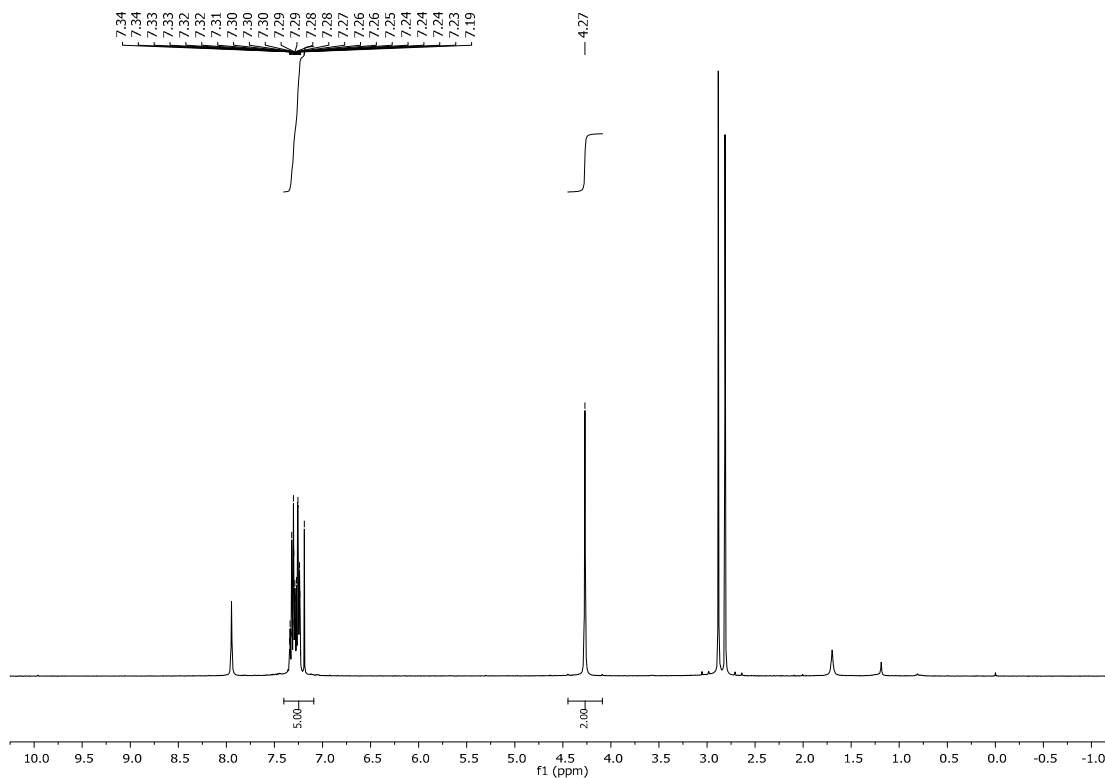
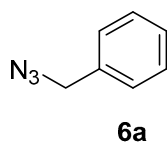


Figure S6. ¹H-NMR spectrum of compound **6a** in accordance with literature. [Zhong, Z.; Chesti, J.; Armstrong, A.; Bull, J.A. Synthesis of Sulfoximine Propargyl Carbamates under Improved Conditions for Rhodium Catalyzed Carbamate Transfer to Sulfoxides *J. Org. Chem.* **2022** *87*, 16115-16126; doi: 10.1021/acs.joc.2c02083B.]

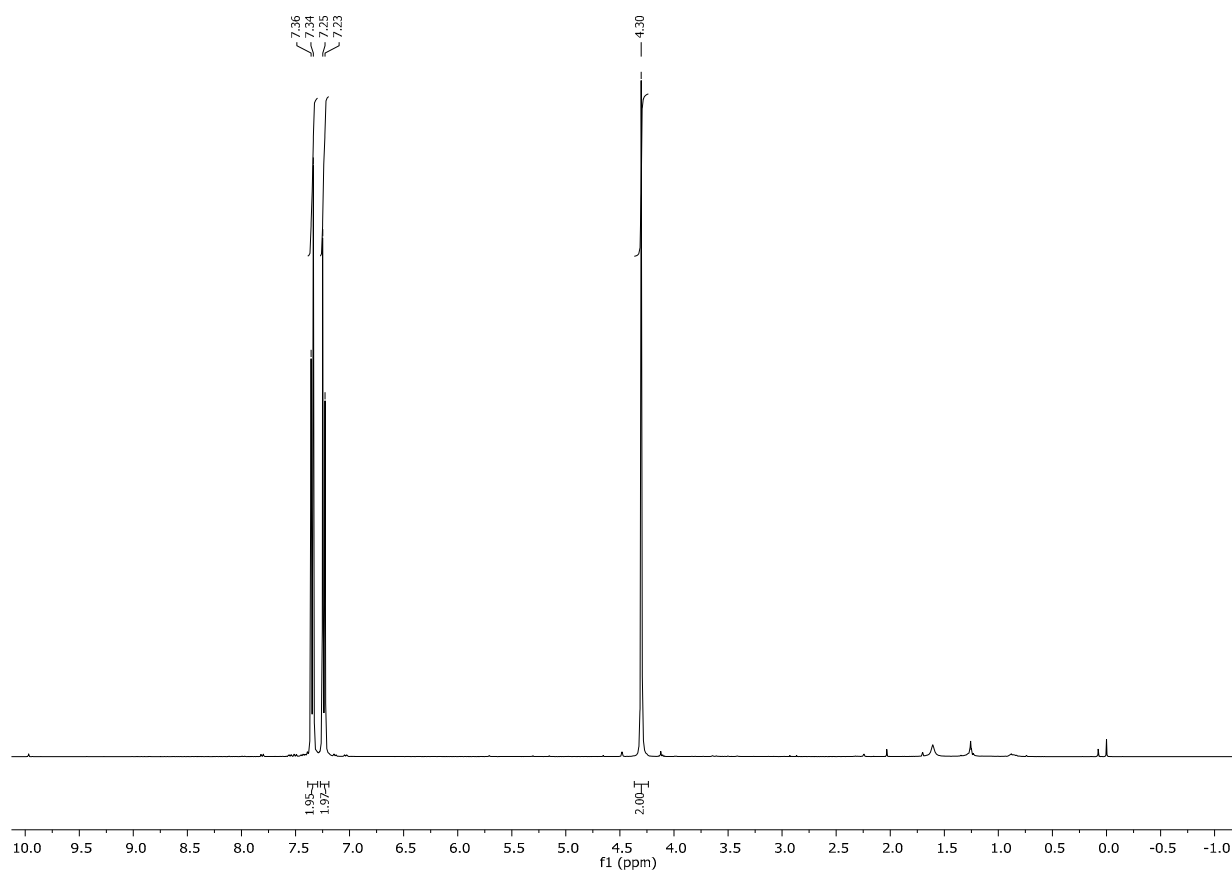
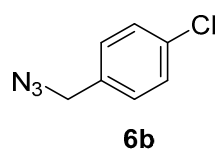


Figure S7. ¹H-NMR spectrum of compound **6b** in accordance with literature. [Vairoletti, F.; Paulino, M.; Mahler, G.; Salinas, G.; Saiz, C. Structure-Based Bioisosterism Design, Synthesis, Biological Evaluation and In Silico Studies of Benzamide Analogs as Potential Anthelmintics. *Molecules* **2022**, *27*, 2659; doi: 10.3390/molecules27092659.]

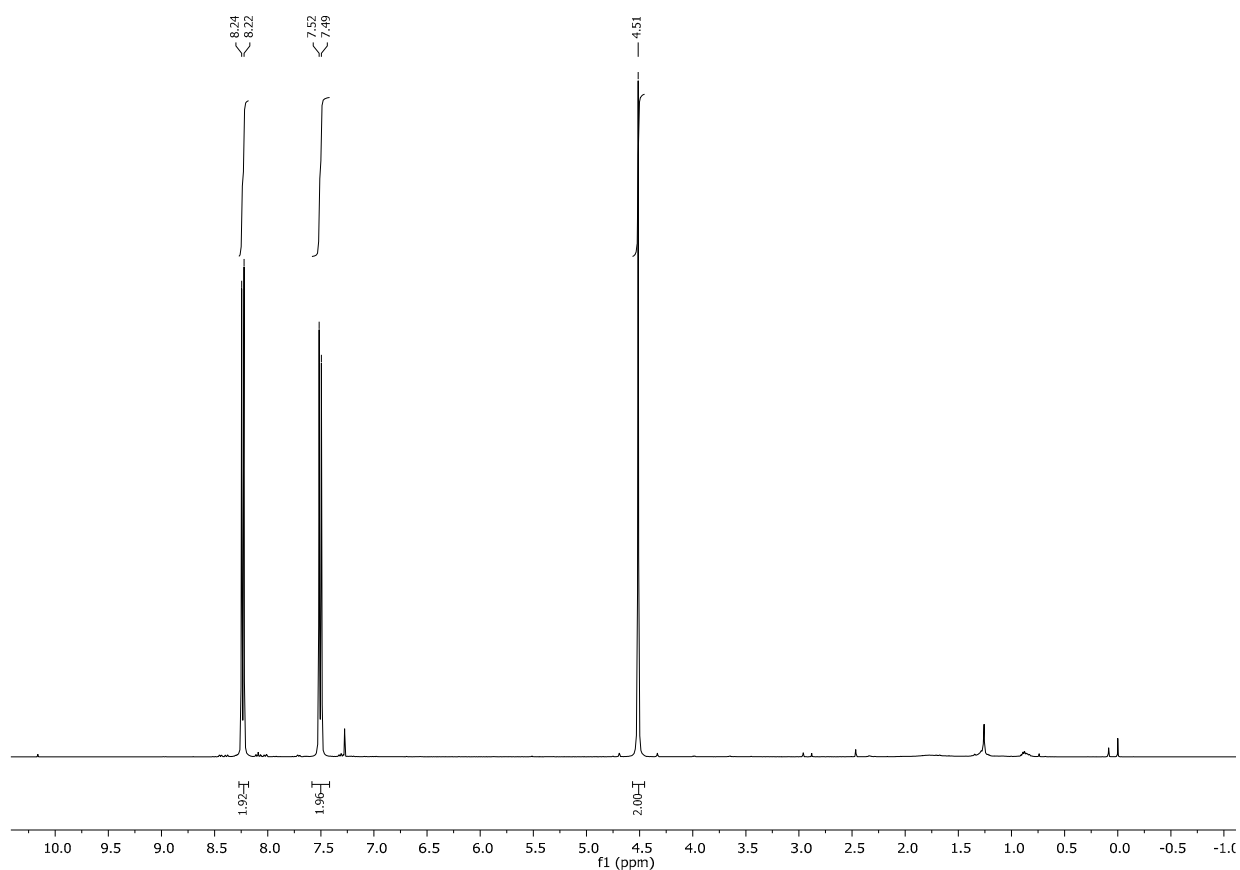
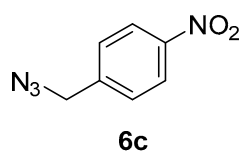


Figure S8. ^1H -NMR spectrum of compound **6c** in accordance with literature. [Rabet, P.T.G.; Fumagalli, G.; Boyd, S.; Greaney, M.F. Benzylic C–H Azidation Using the Zhdankin Reagent and a Copper Photoredox Catalyst, *Org. Lett.* **2016** *18*, 1646-1649; doi: 10.1021/acs.orglett.6b00512.]

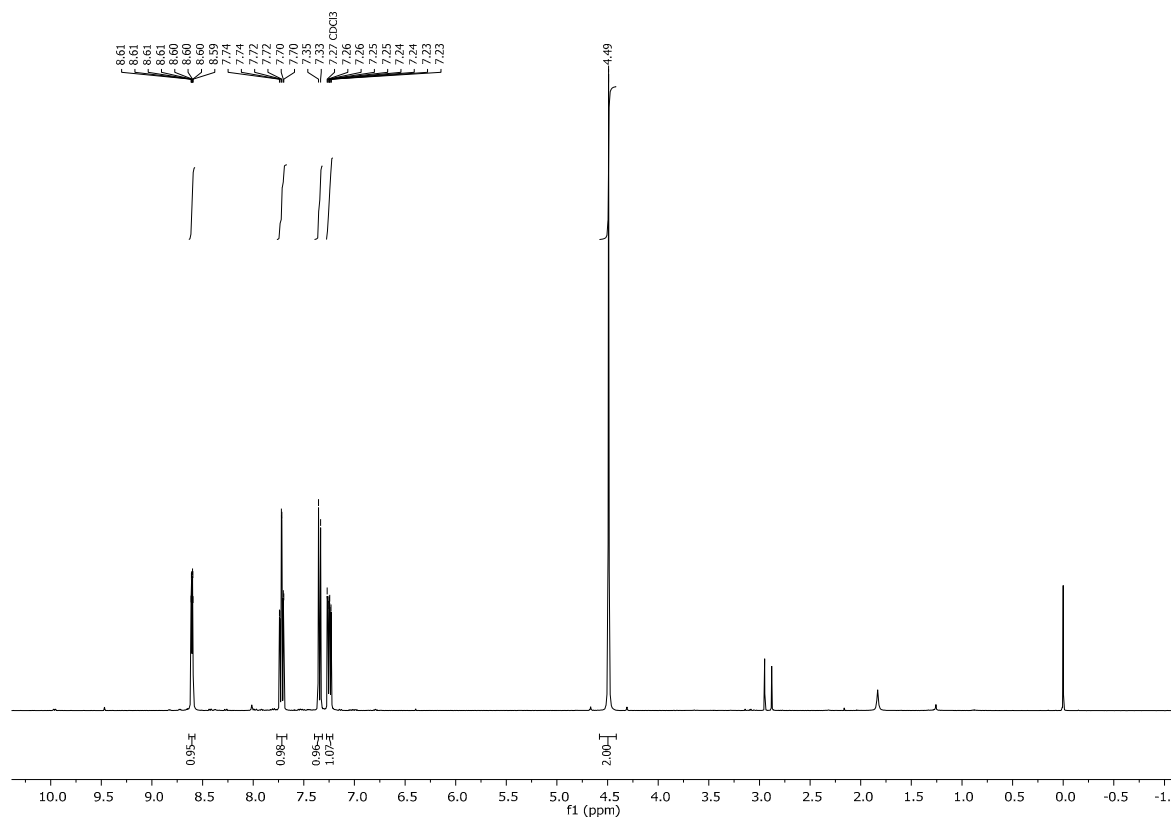
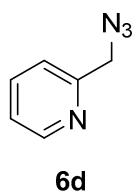


Figure S9. ^1H -NMR spectrum of compound **6d** in accordance with literature. [Sacchetti, A.; Urra-Mancilla, C.; Colombo Dugoni, G. Synthesis of DPA-triazole structures and their application as ligand for metal catalyzed organic reactions, *Tetrahedron*, **2022**, 132581; doi: 10.1016/j.tet.2021.132581.]

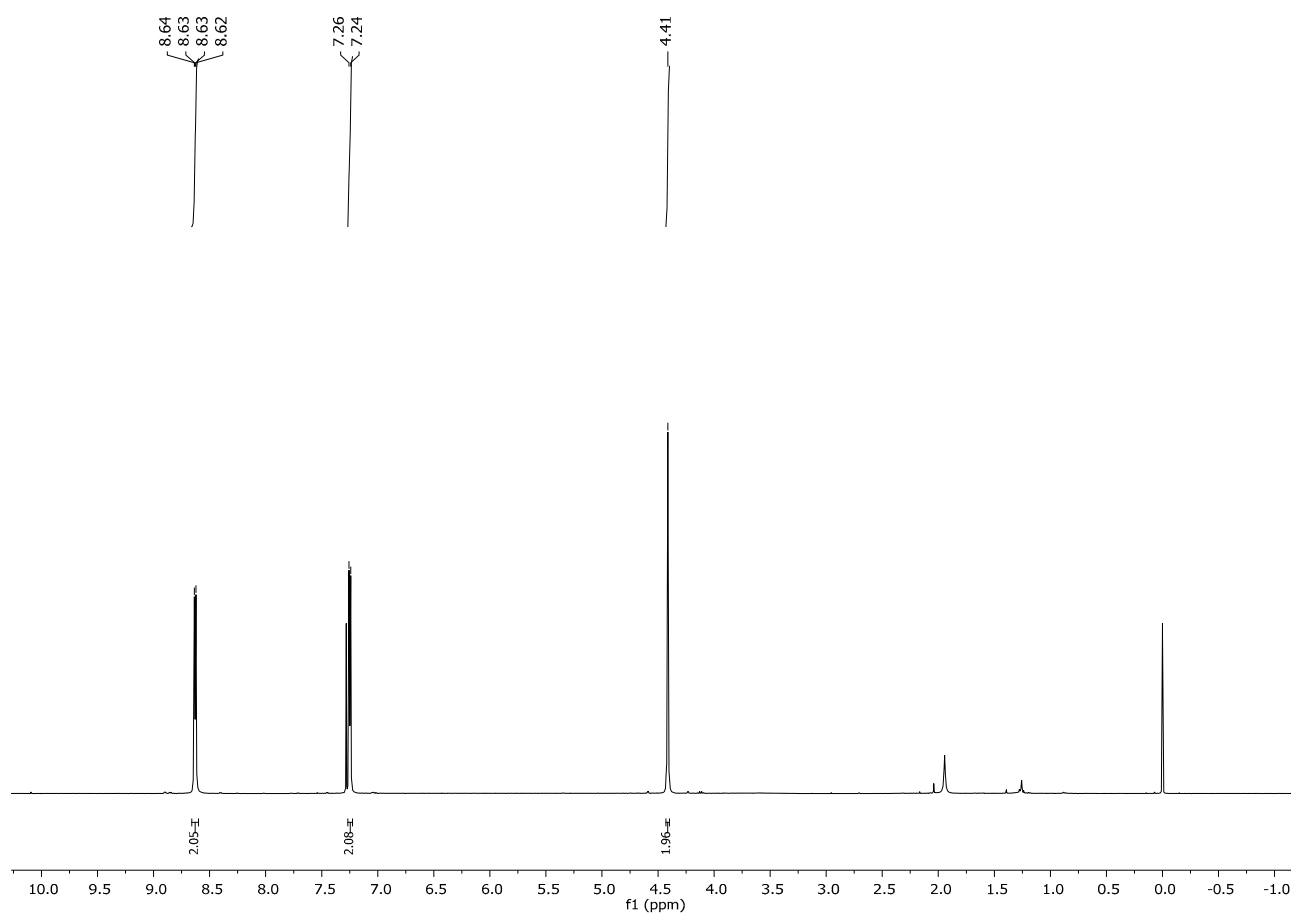
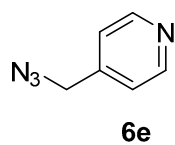


Figure S10. ^1H -NMR spectrum of compound **6e** in accordance with literature. [Sacchetti, A.; Urra-Mancilla, C.; Colombo Dugoni, G. Synthesis of DPA-triazole structures and their application as ligand for metal catalyzed organic reactions, *Tetrahedron*, **2022**, 132581; doi: 10.1016/j.tet.2021.132581.]

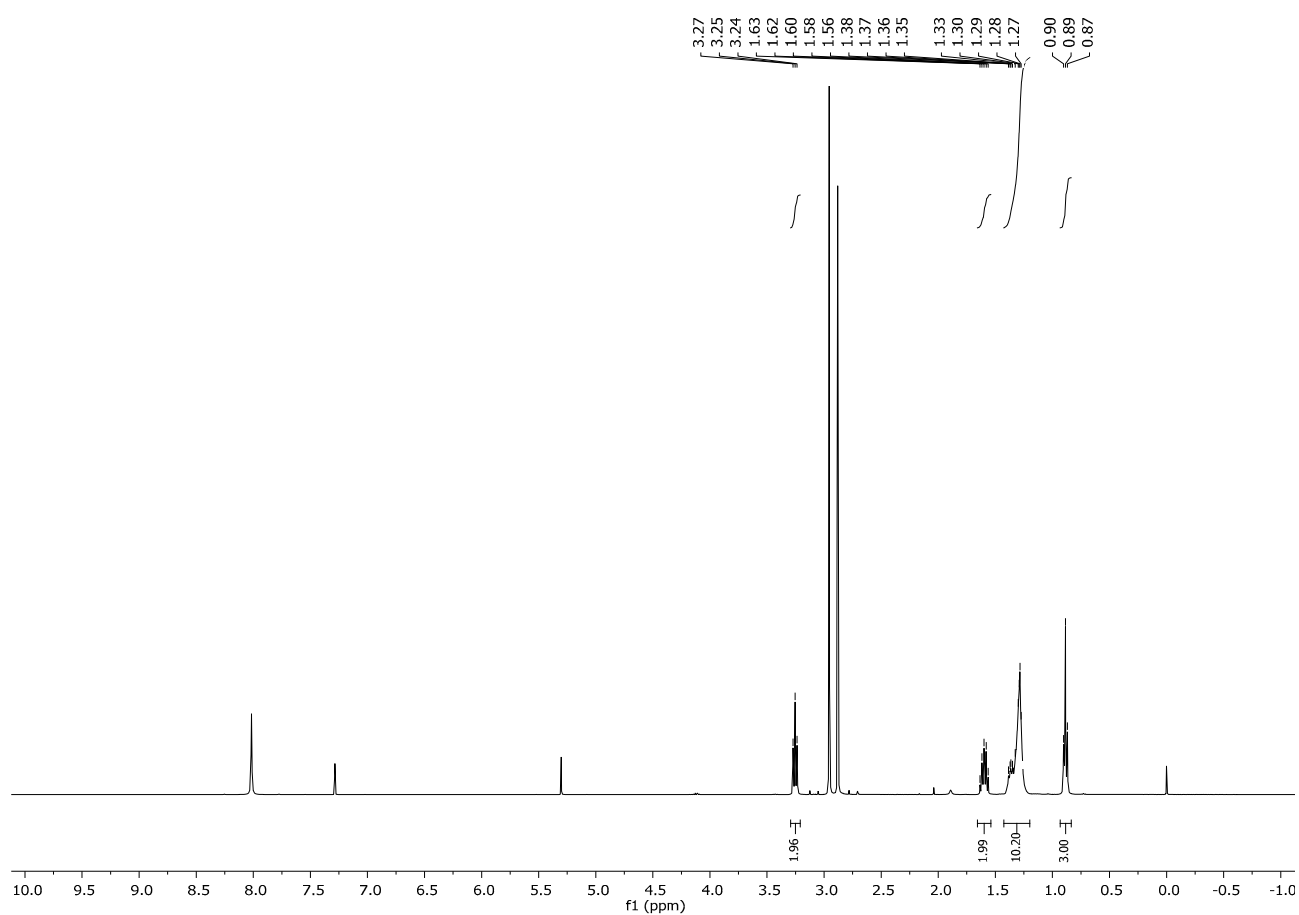
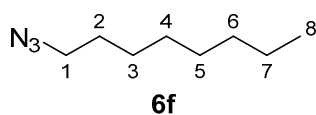


Figure S11. ^1H -NMR spectrum of compound **6f** in accordance with literature. [Proietti, G.; Prathap, K.J.; Ye, X.; Olsson, R.T.; Dinér, P. Nickel Boride Catalyzed Reductions of Nitro Compounds and Azides: Nanocellulose-Supported Catalysts in Tandem Reactions. *Synthesis* **2022**; 54, 133-146; doi: 10.1055/a-1579-2190.]

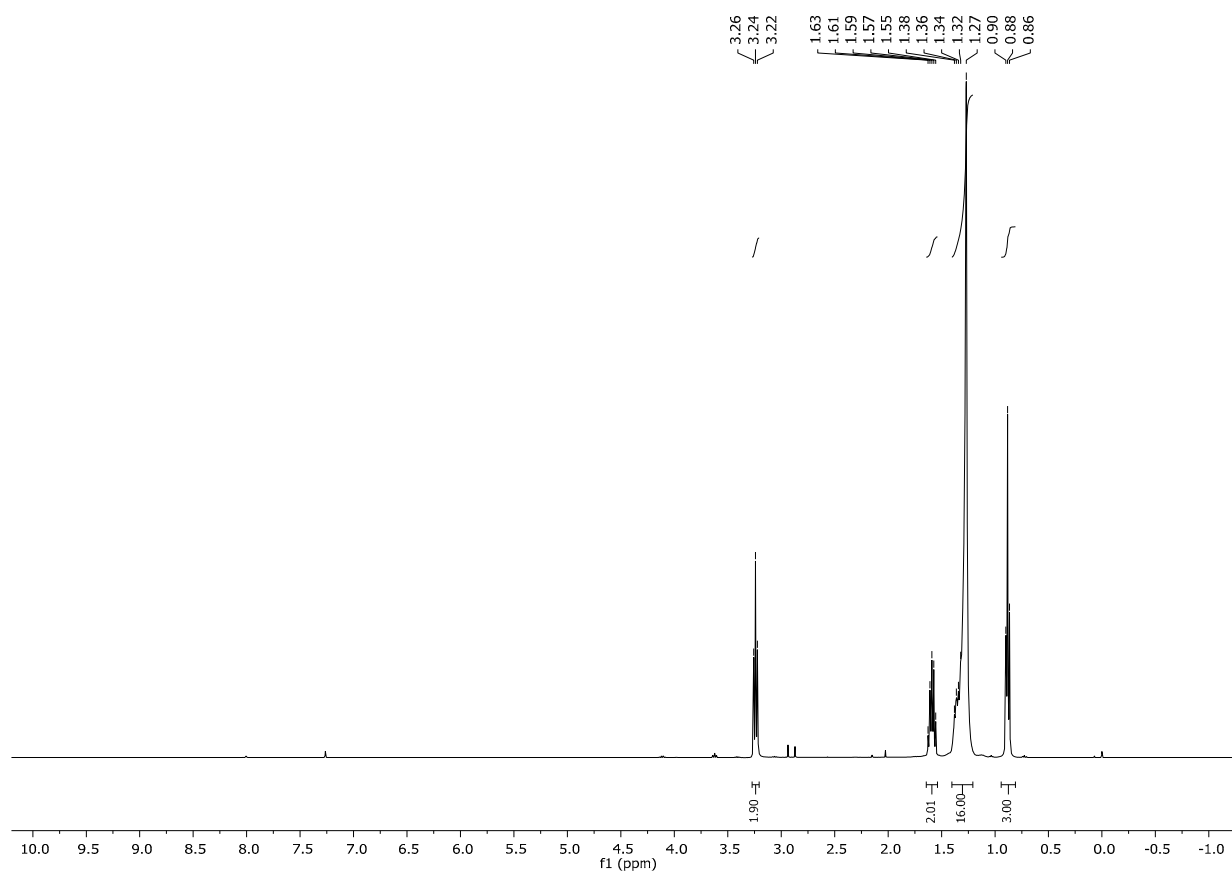
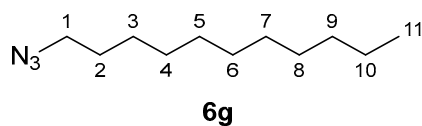


Figure S12. ^1H -NMR spectrum of compound **6g** in accordance with literature. [Natarajan, B.; Jayaraman, N. Synthesis and studies of Rh(I) catalysts within and across poly(alkyl aryl ether) dendrimers, *J. Organometallic Chem.*, 696, **2011**, 722-730; doi: 10.1016/j.jorganchem.2010.09.054.]

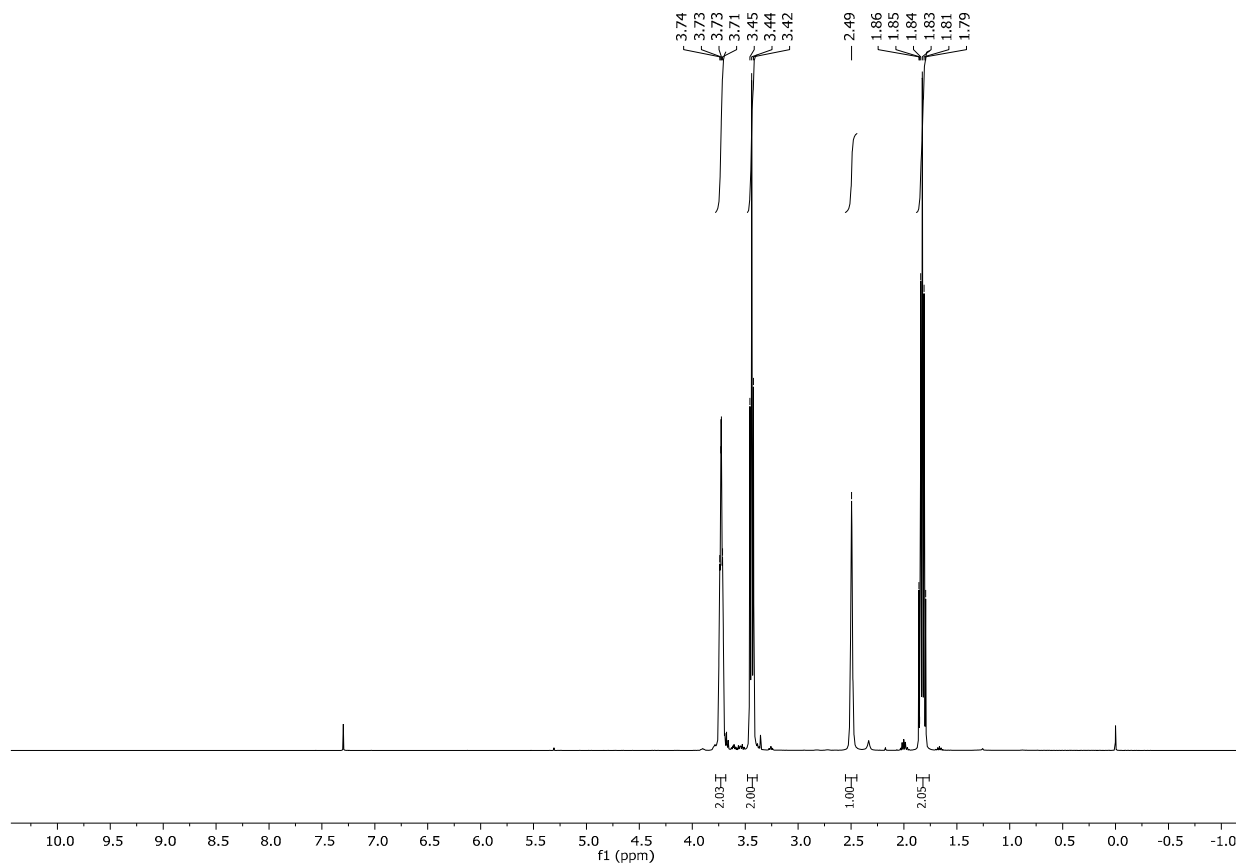
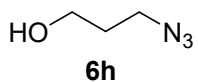


Figure S13. ¹H-NMR spectrum of compound **6h** in accordance with literature. [Macerata, E.; Mossini, E.; Scaravaggi, S.; Mariani, M.; Mele, A.; Panzeri, W.; Boubals, N.; Berthon, L.; Charbonnel, M-C.; Sansone, F.; Arduini, A.; Casnati, A. Hydrophilic Clicked 2,6-Bis-triazolyl-pyridines Endowed with High Actinide Selectivity and Radiochemical Stability: Toward a Closed Nuclear Fuel Cycle *J. Am. Chem. Soc.* **2016** 138 (23), 7232-7235; doi: 10.1021/jacs.6b03106.]

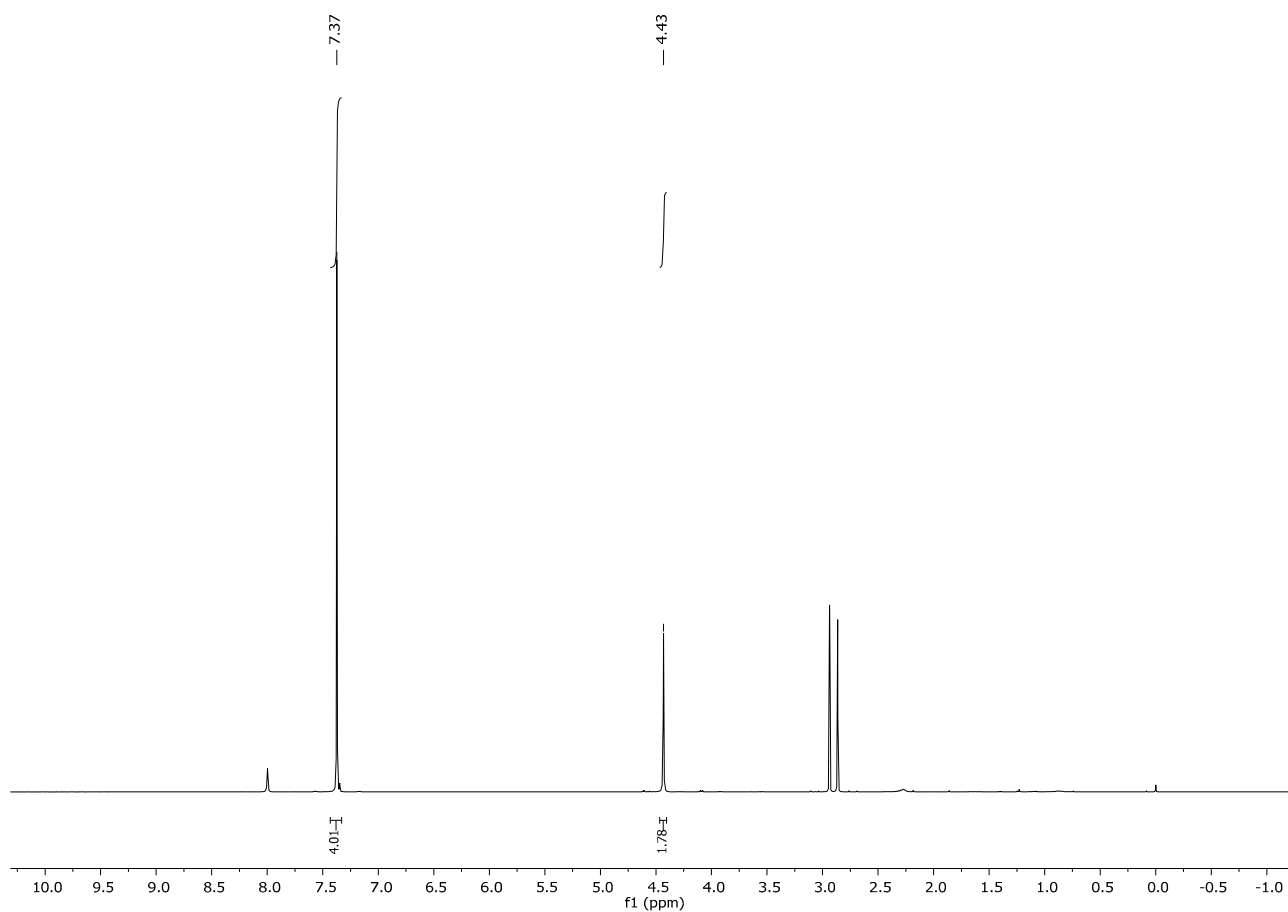
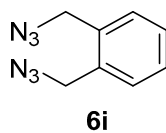


Figure S14. ^1H -NMR spectrum of compound **6i** in accordance with literature. [Guo, Z.-F.; Yan, H.; Li, Z.-F.; Lu, Z.-L. Synthesis of mono- and di-[12]aneN₃ ligands and study on the catalytic cleavage of RNA model 2-hydroxypropyl-p-nitrophenyl phosphate with their metal complexes, *Org. Biomol. Chem.*, **2011**, 9, 6788-6796; doi: 10.1039/C1OB05942D.]

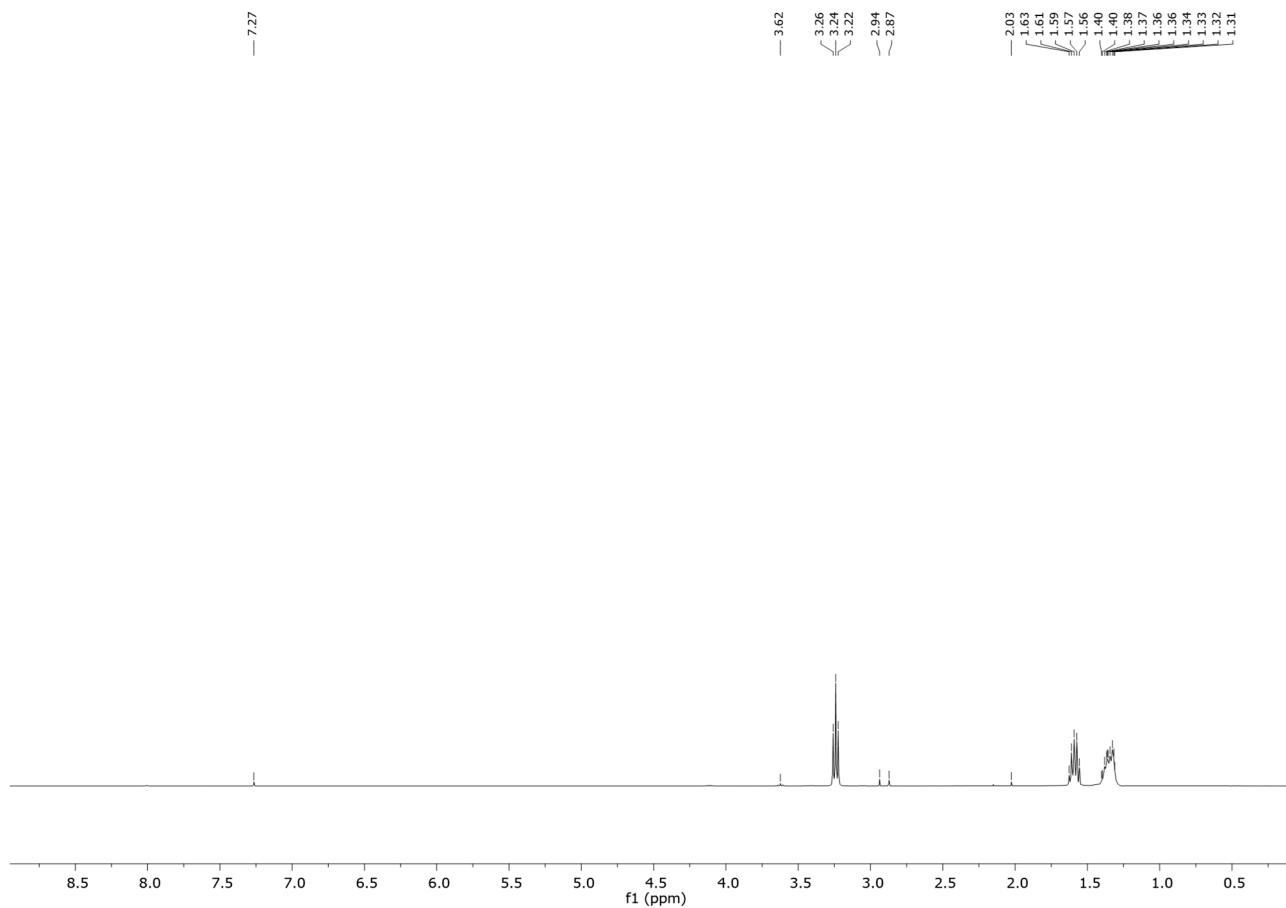
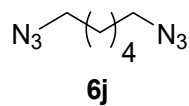
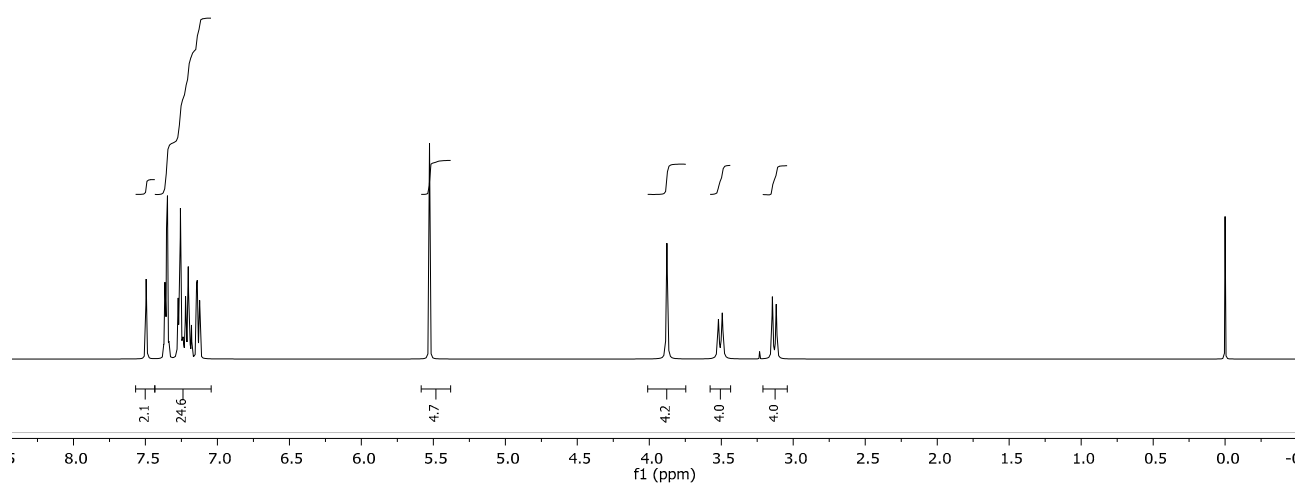
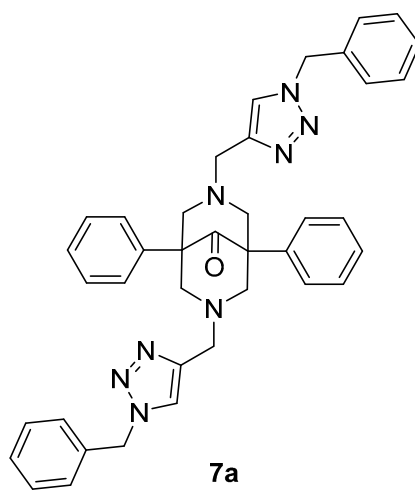


Figure S15. ^1H -NMR spectrum of compound **6j** in accordance with literature. [Peng, L.; Zhao, Y.; Okuda, Y.; Le, L.; Tang, Z.; Yin, S.-F.; Qiu, R.; Orita, A. Process-Divergent Syntheses of 4- and 5-Sulfur-Functionalized 1,2,3-Triazoles via Copper-Catalyzed Azide–Alkyne Cycloadditions of 1-Phosphinyl-2-sulfanylethynes *The Journal of Organic Chemistry* **2023** 88 (5), 3089-3108; doi: 10.1021/acs.joc.2c02876.]



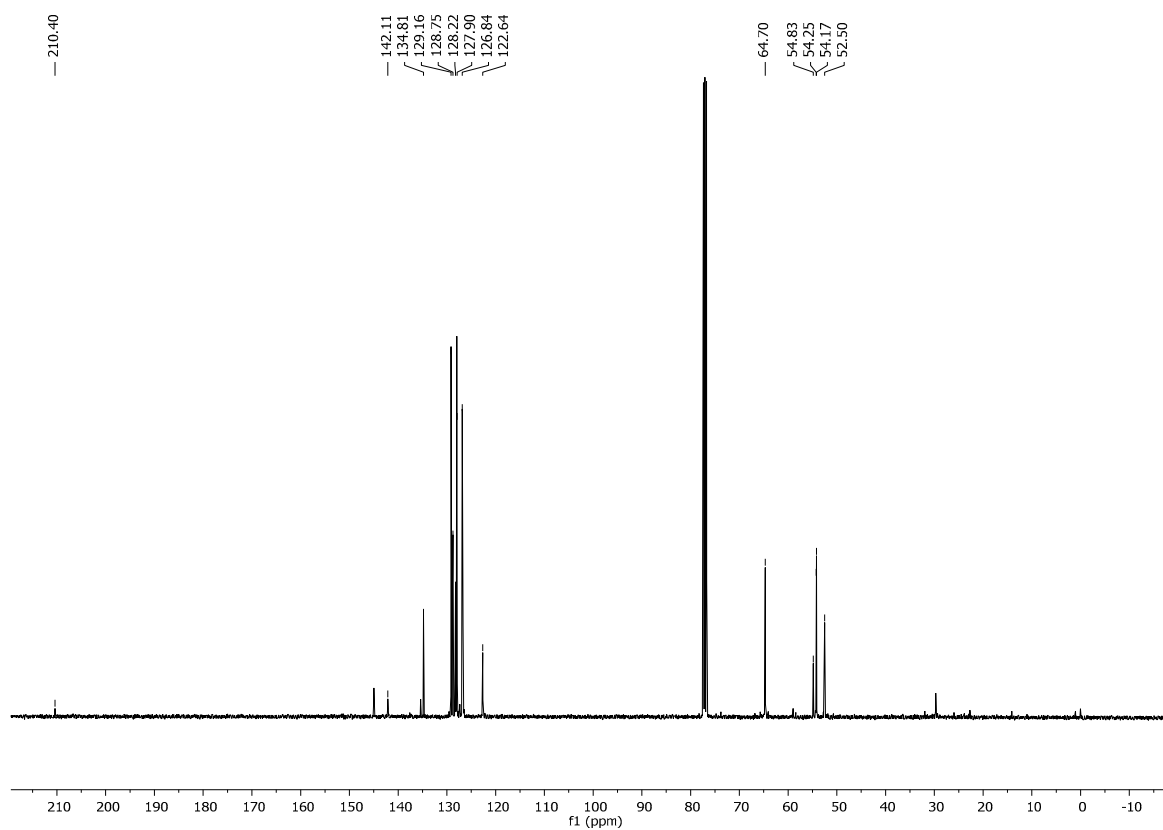
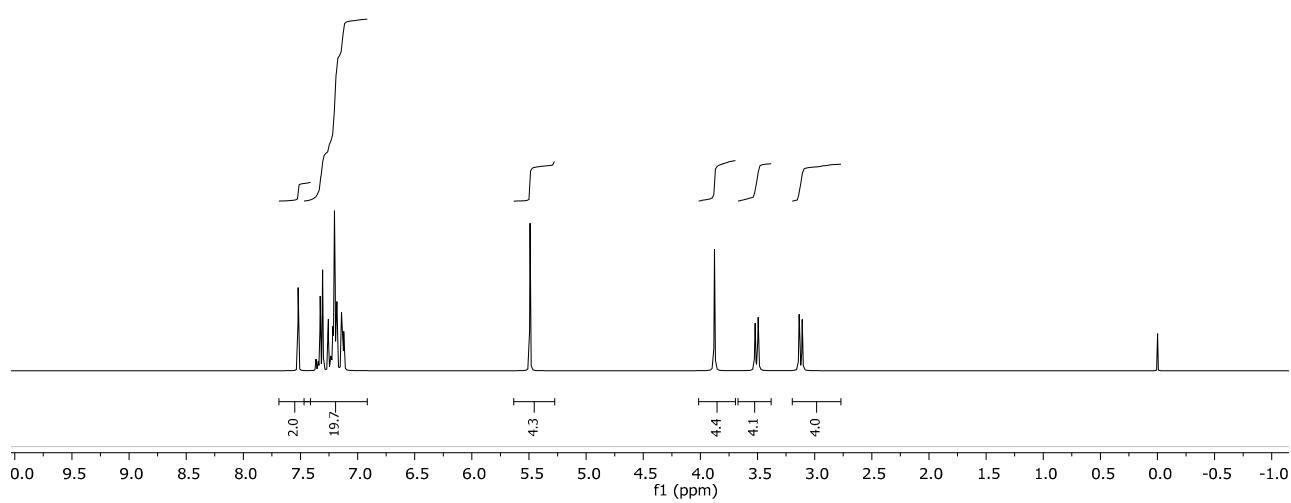
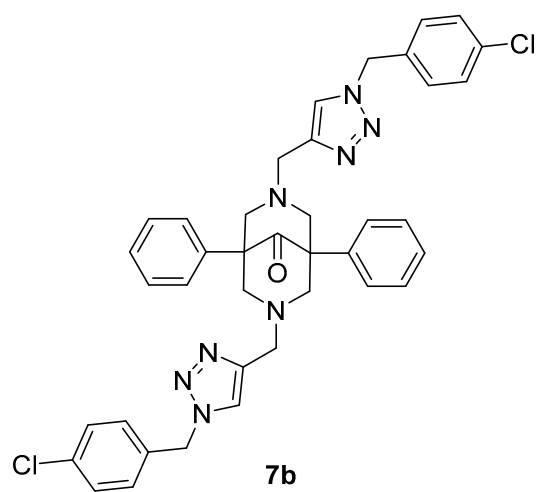


Figure S16. ¹H and ¹³C-NMR spectra of compound **7a**.



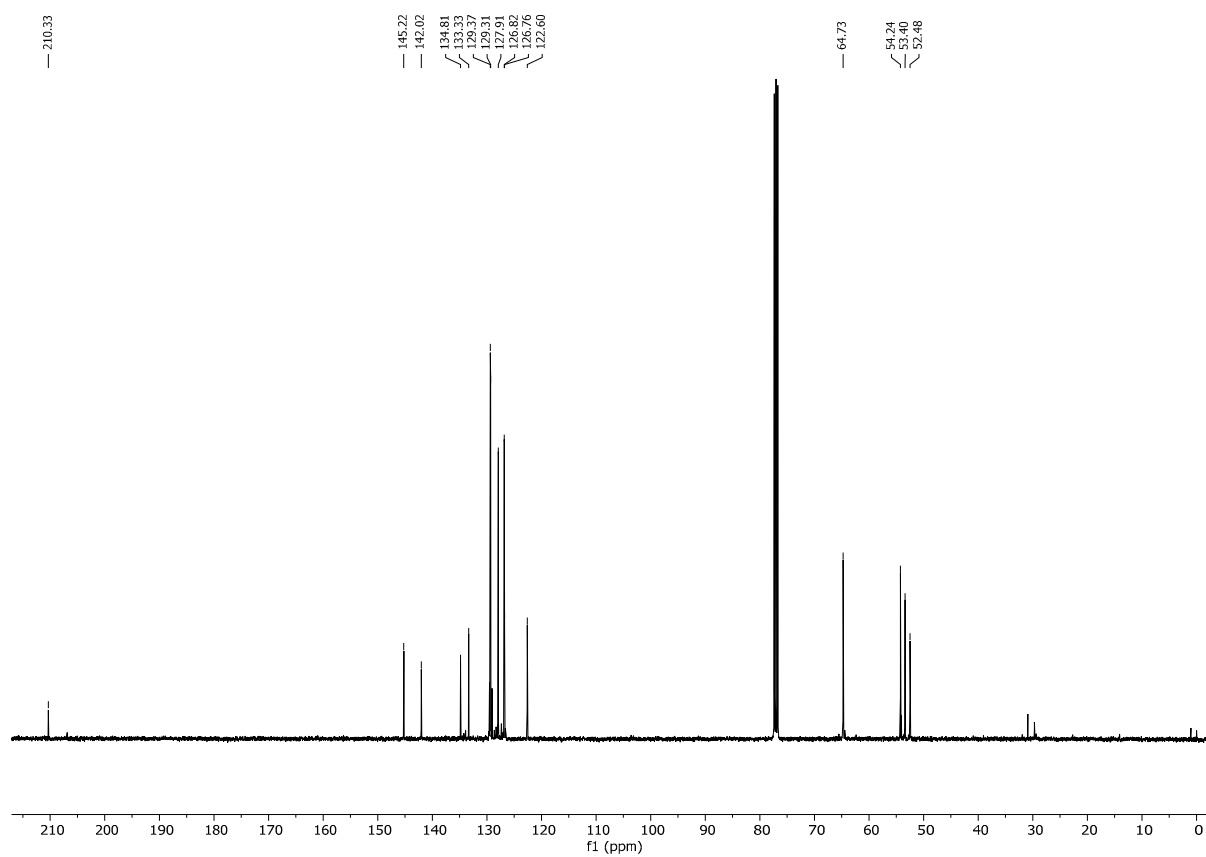
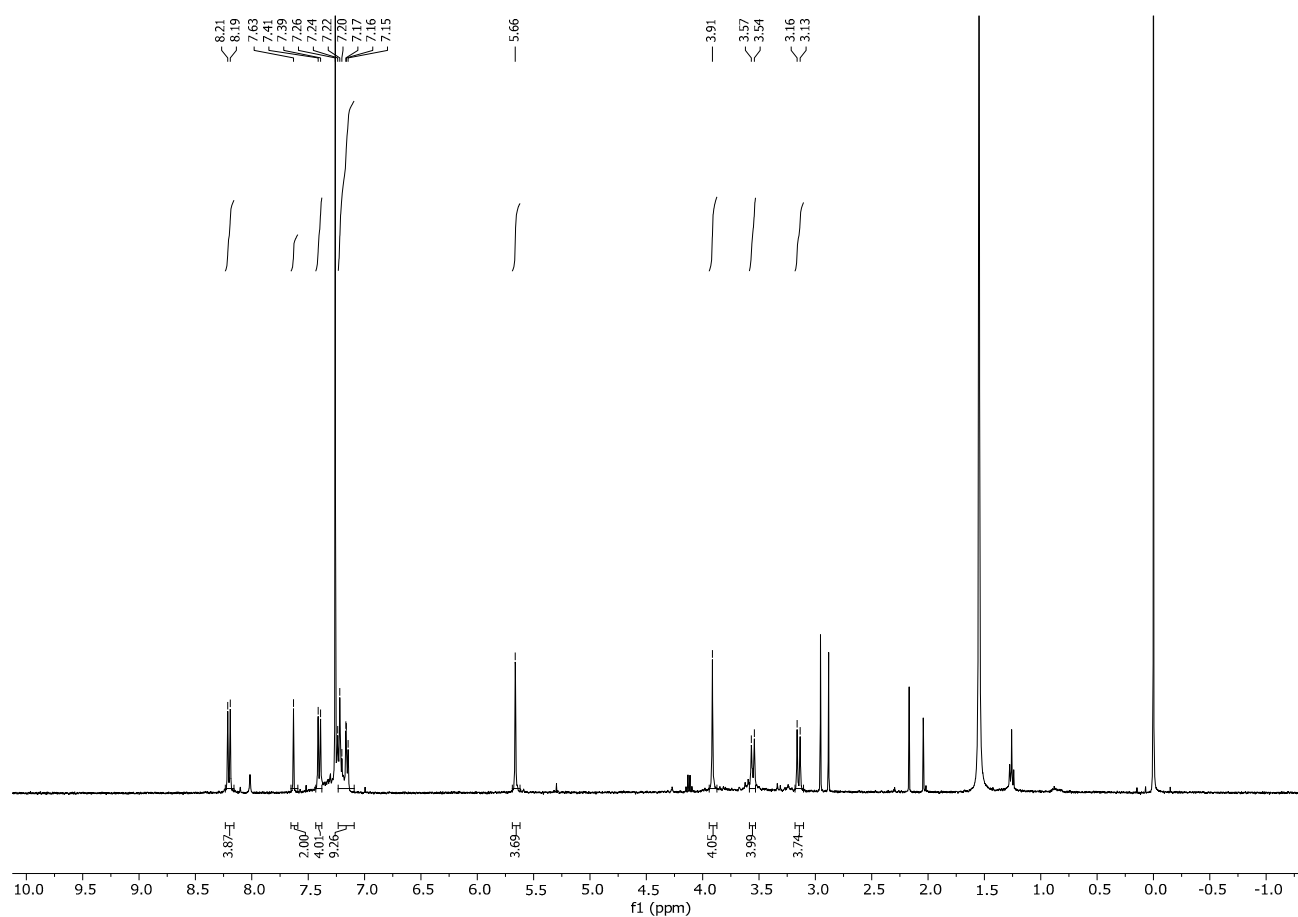
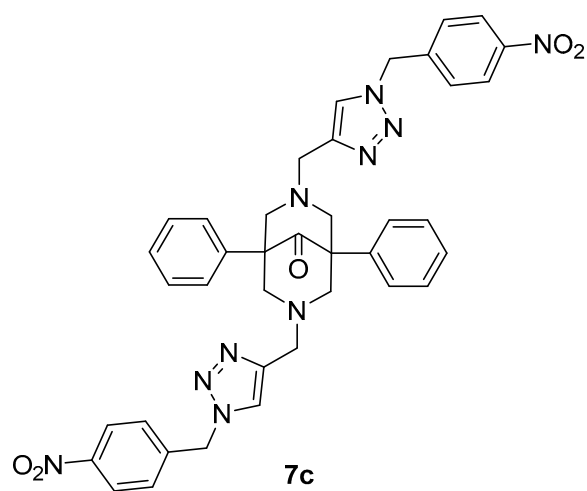


Figure S17. ^1H and ^{13}C -NMR spectra of compound **7b**.



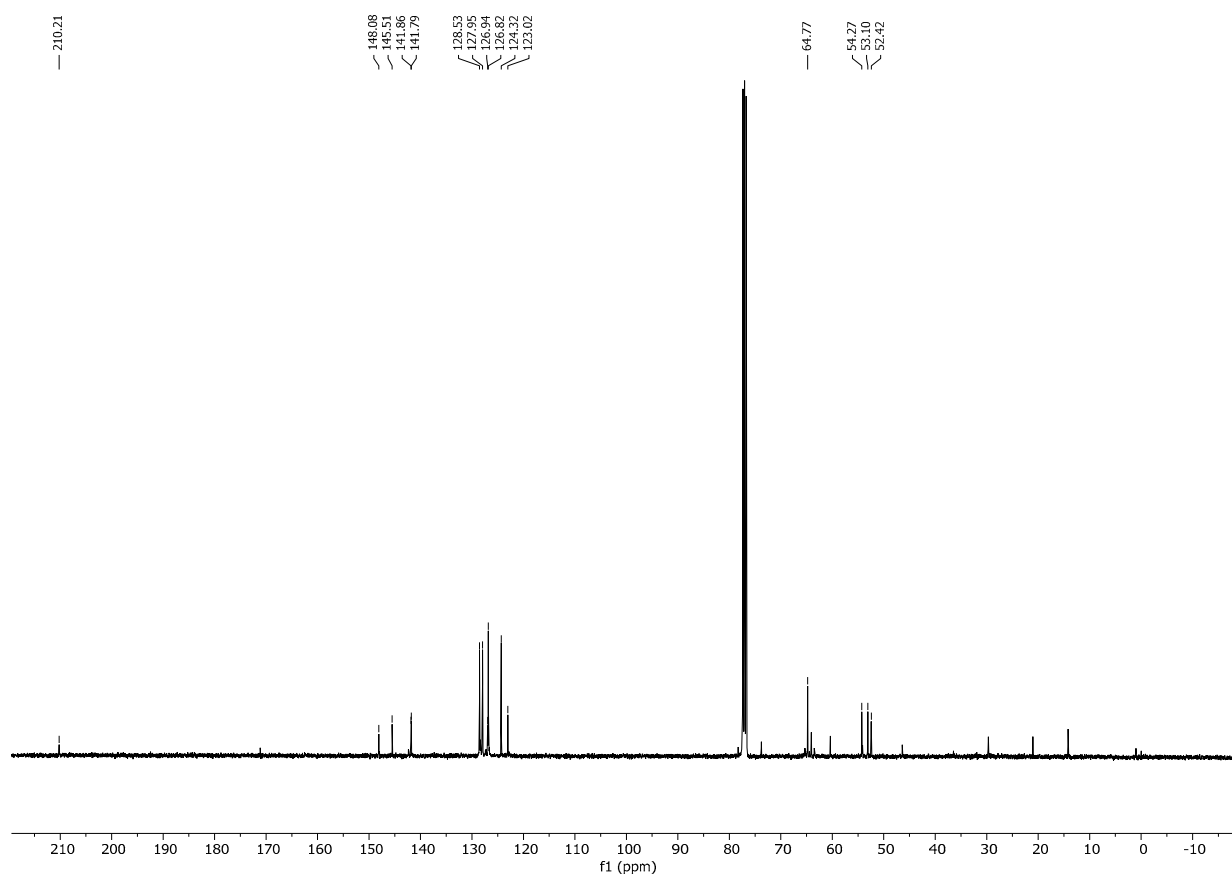
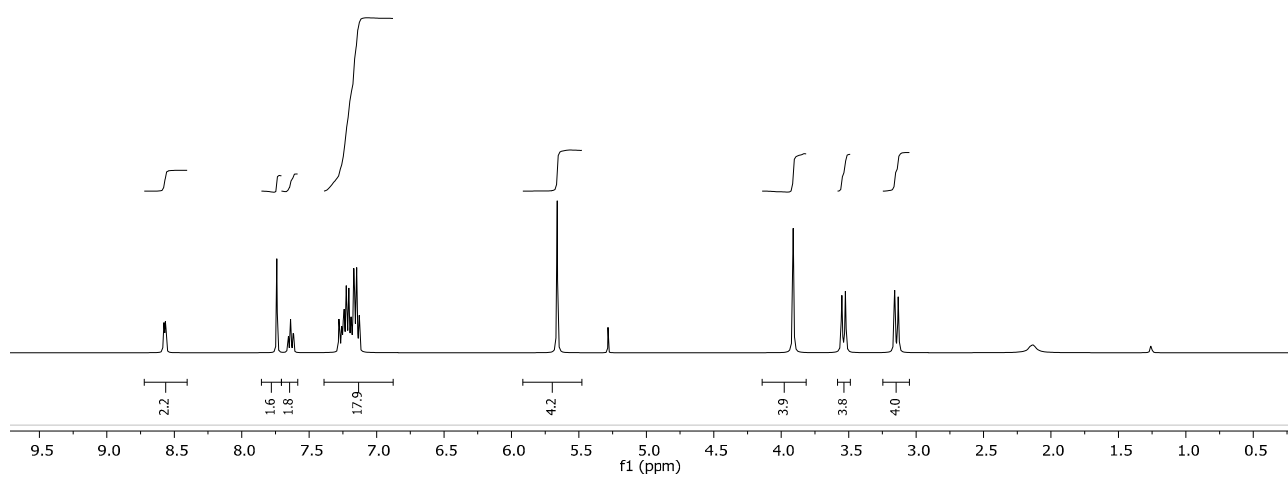
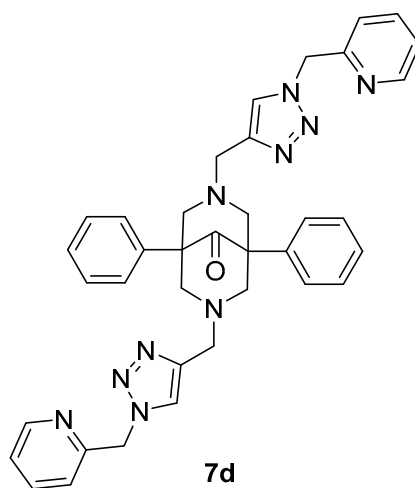


Figure S18. ^1H and ^{13}C -NMR spectra of compound **7c**.



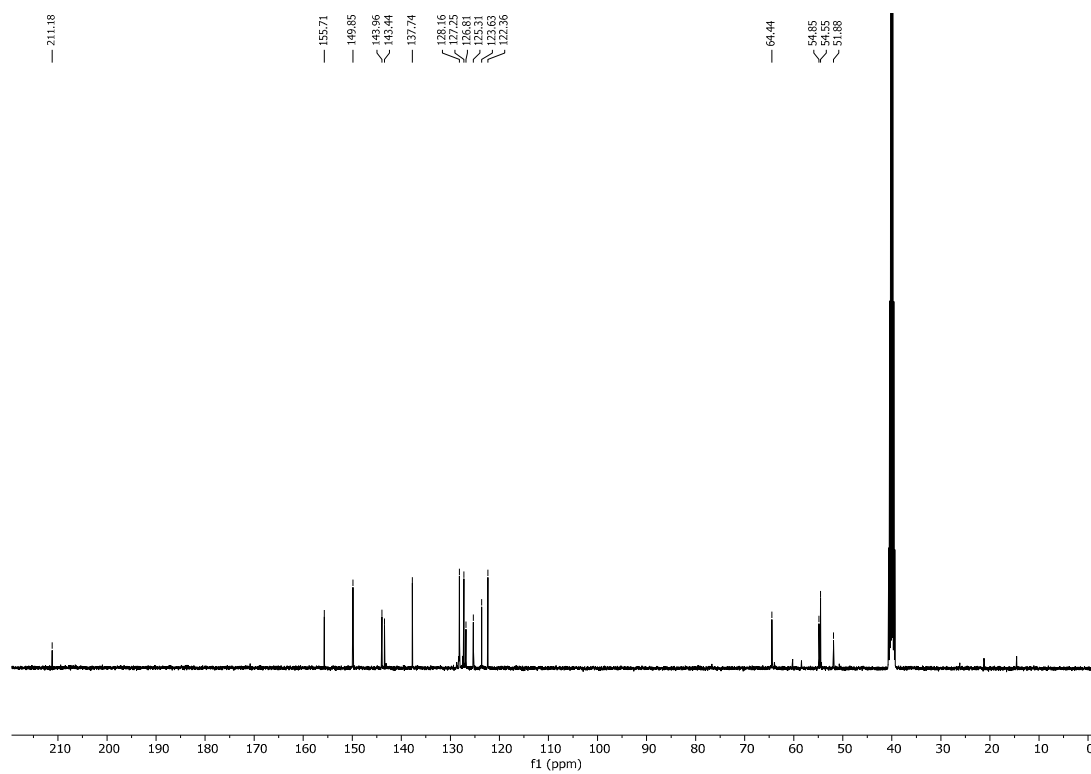
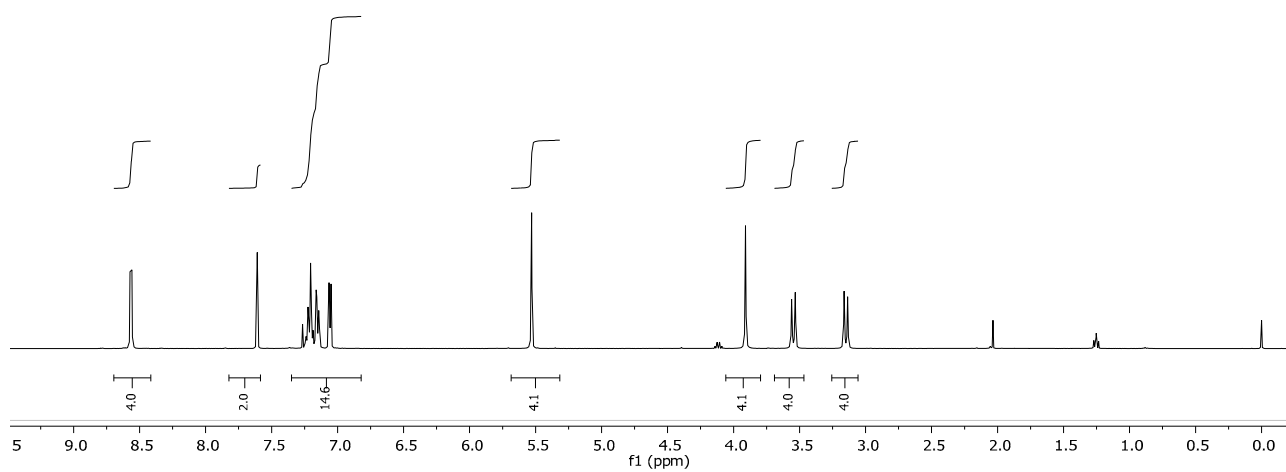
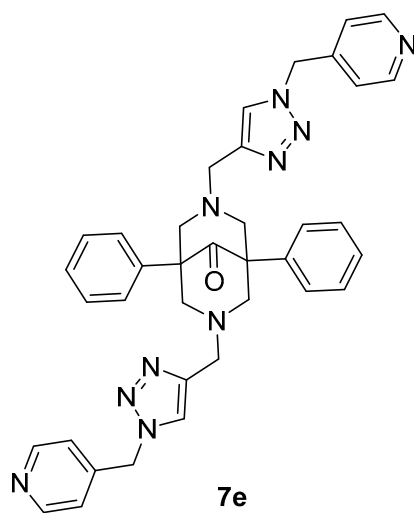


Figure S19. ^1H and ^{13}C -NMR spectra of compound **7d**.



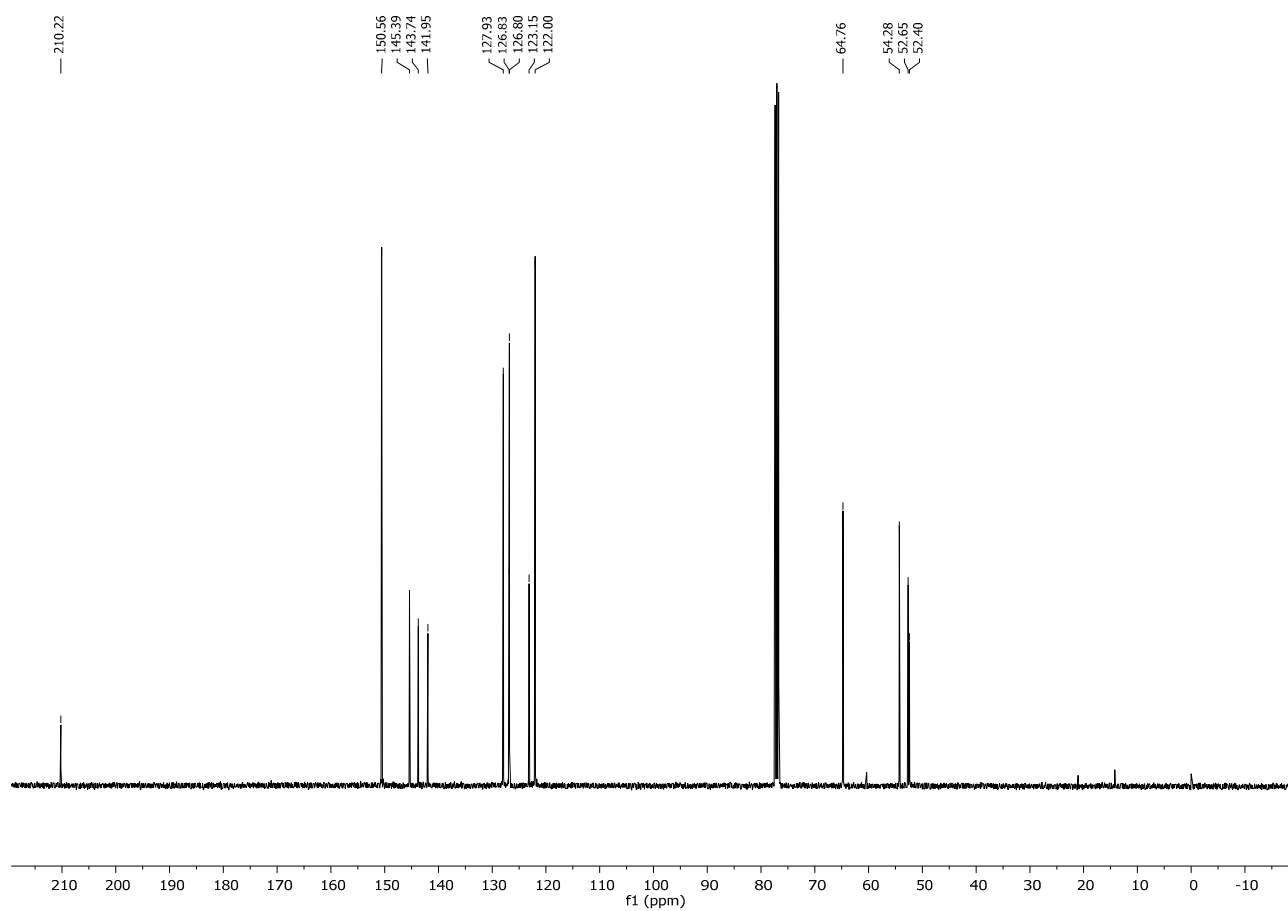
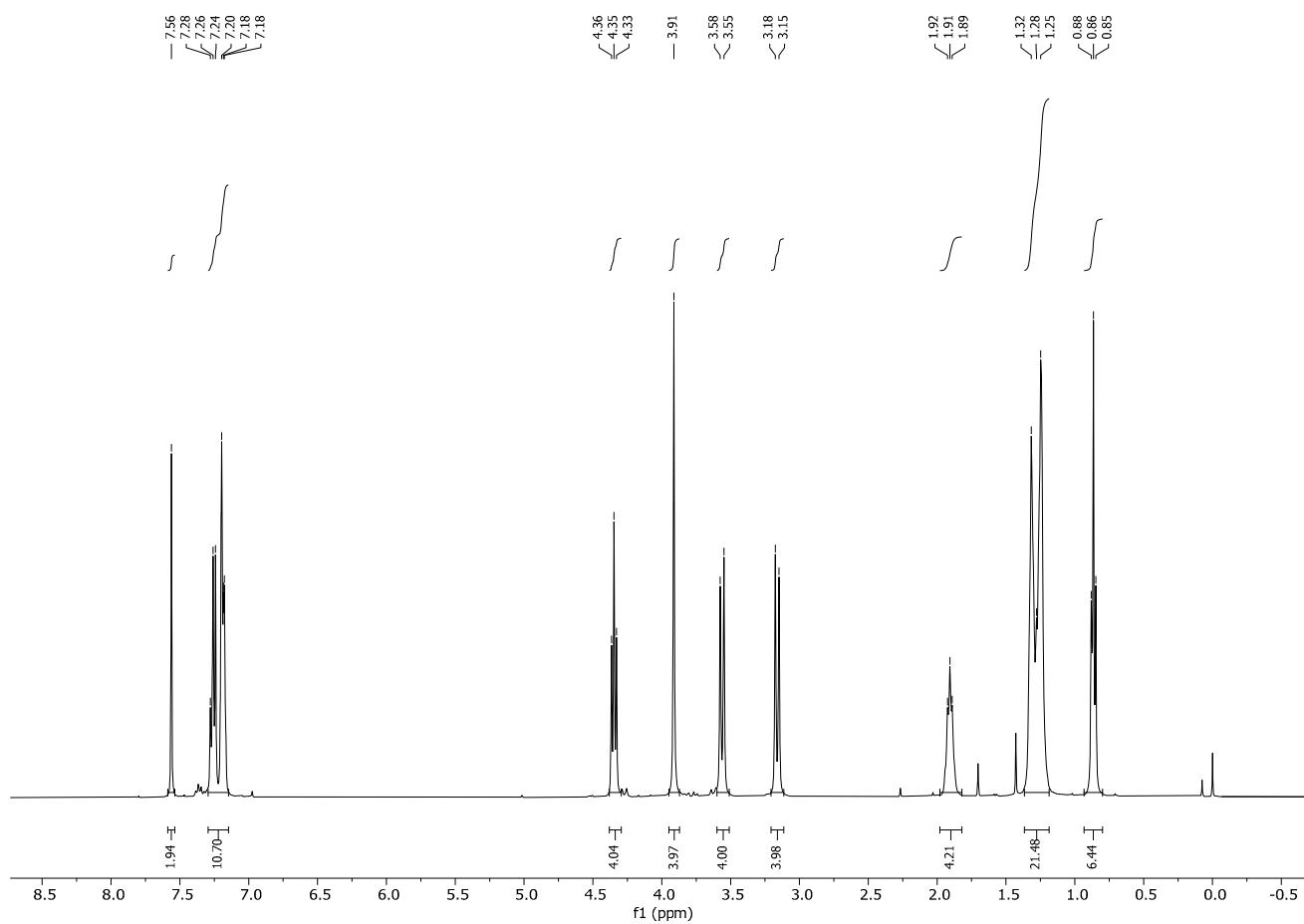
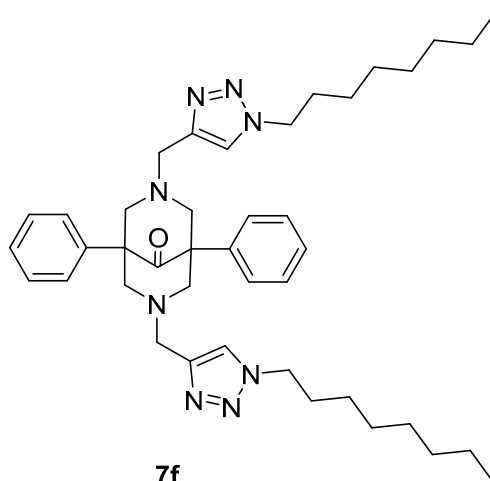


Figure S20. ¹H and ¹³C-NMR spectra of compound **7e**.



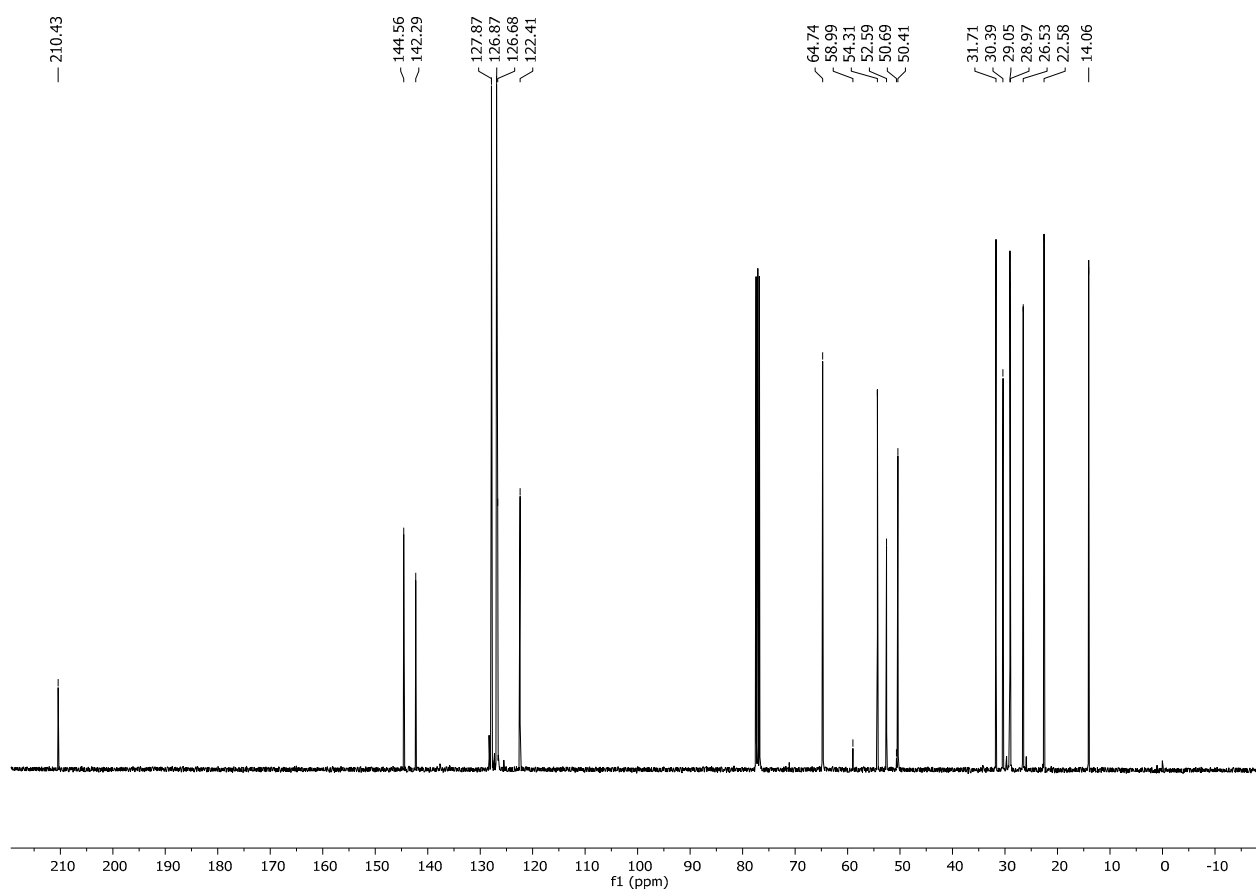
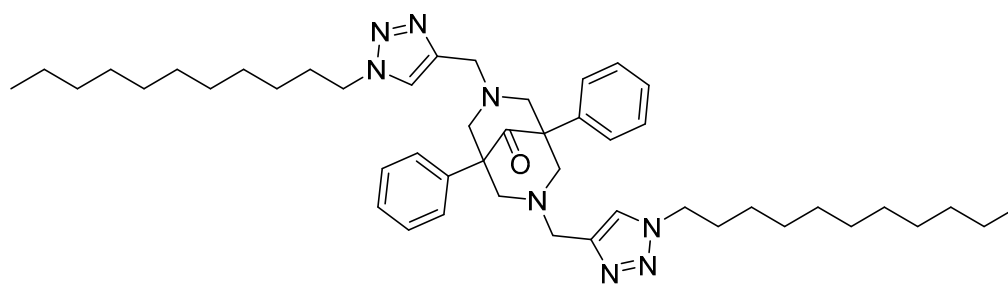
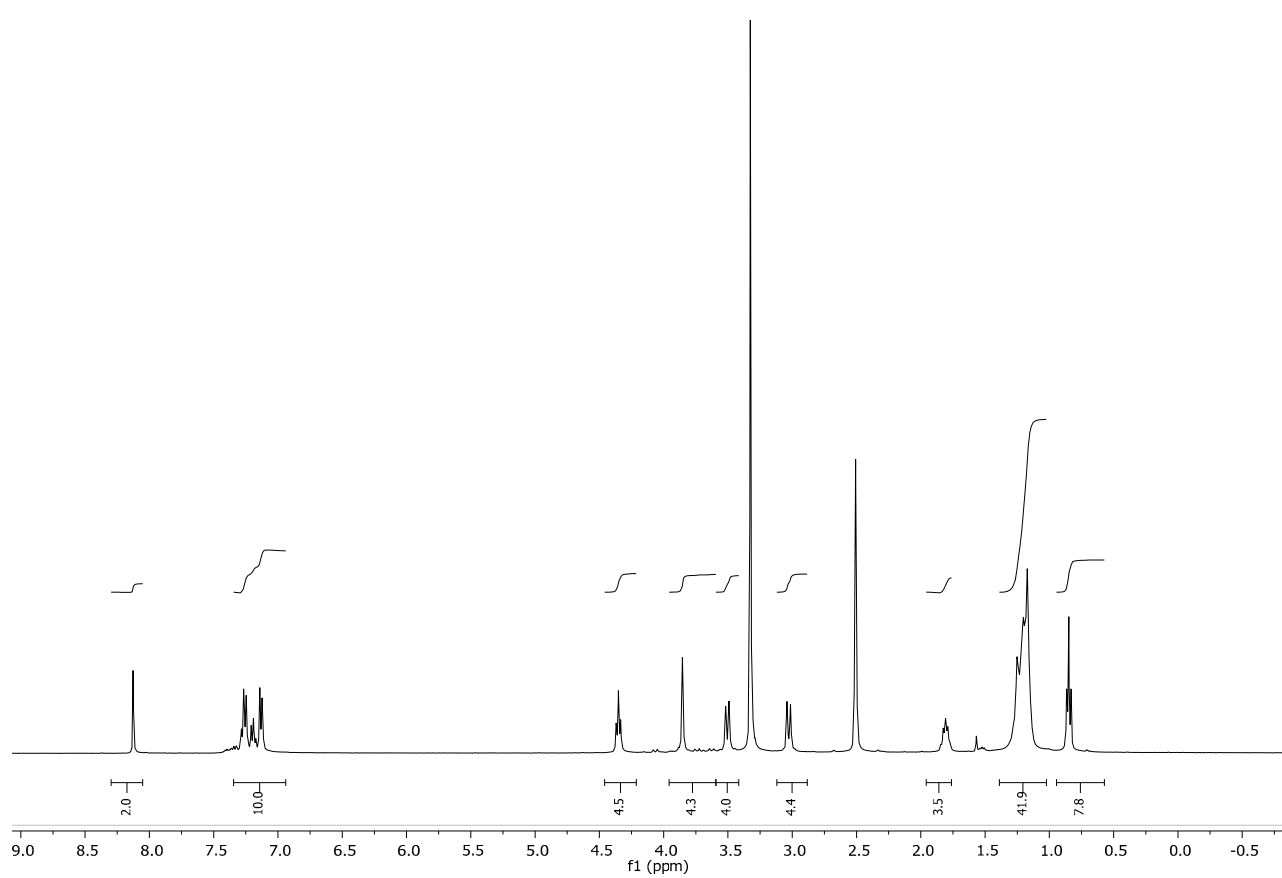


Figure S21. ^1H and ^{13}C -NMR spectra of compound **7f**.



7g



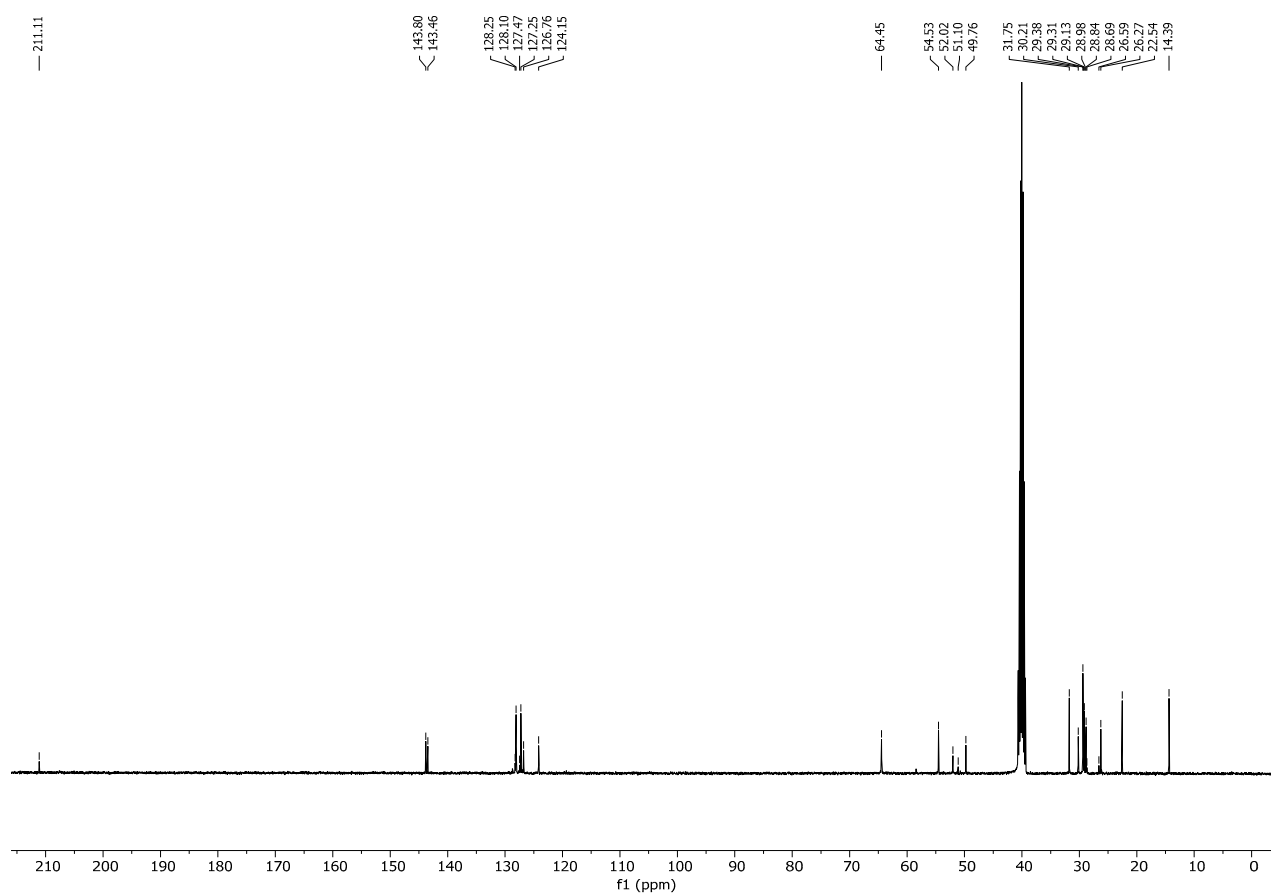
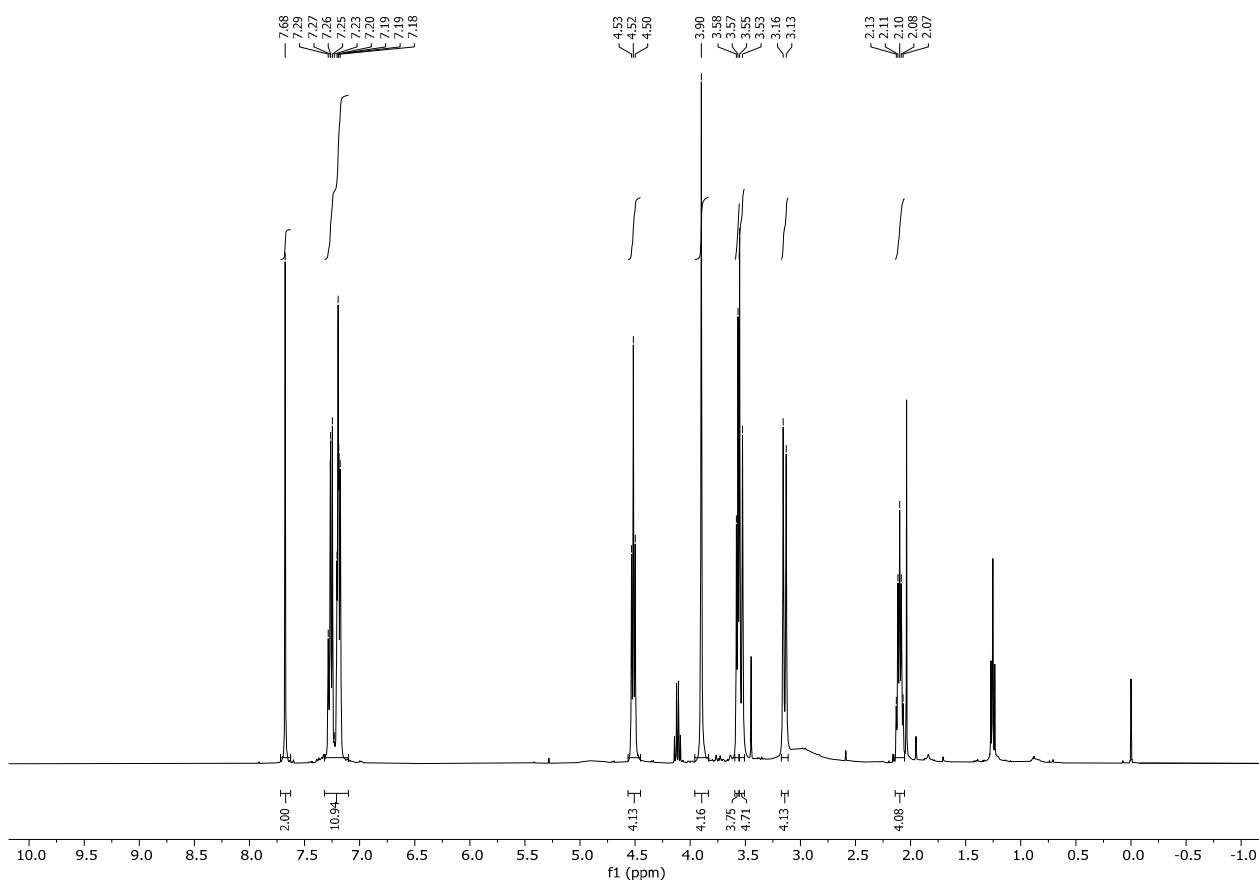
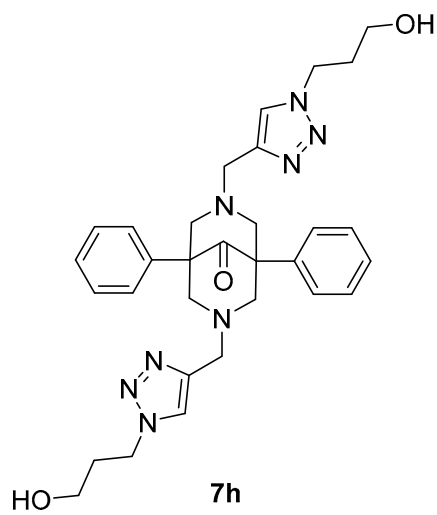


Figure S22. ^1H and ^{13}C -NMR spectra of compound **7g**.



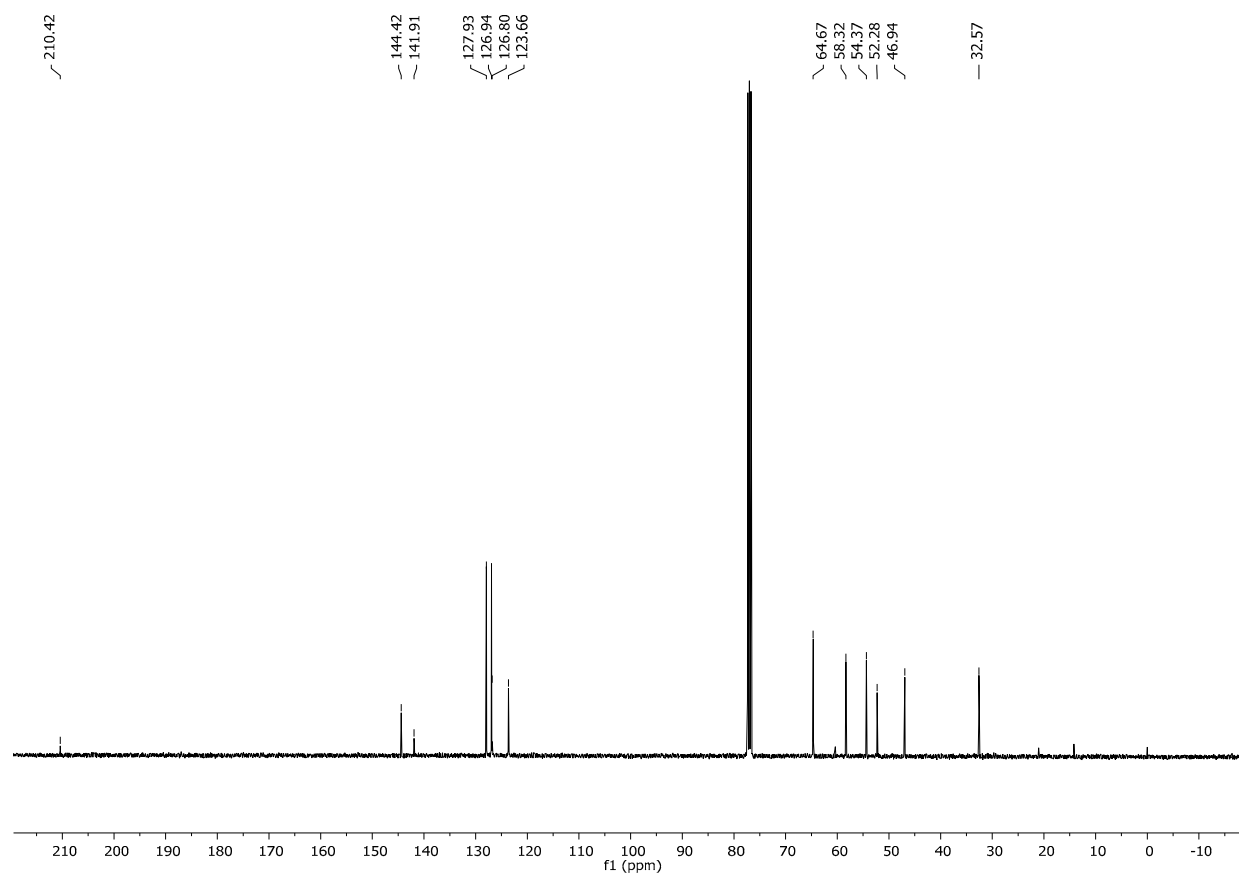
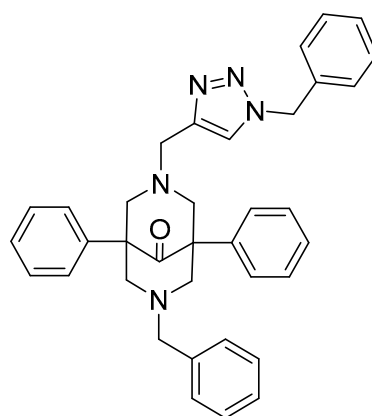
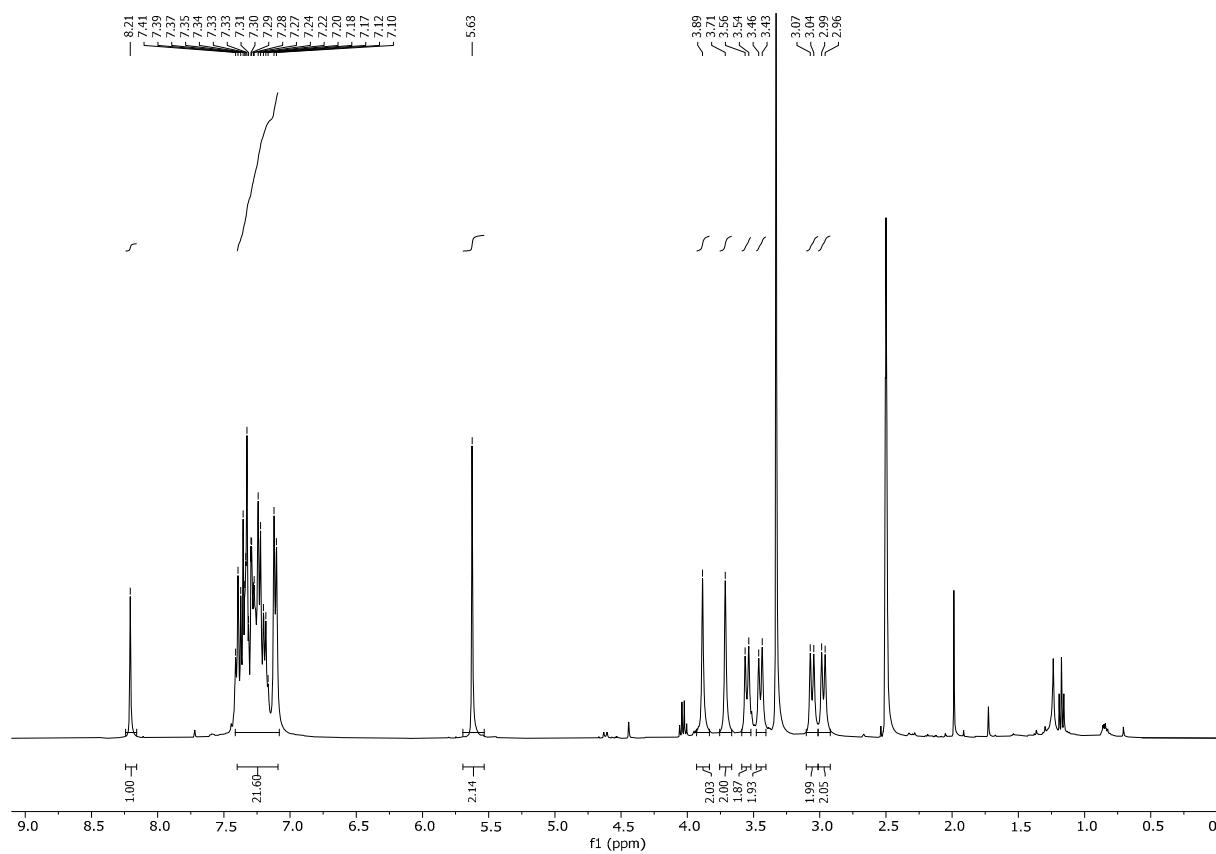


Figure S23. ¹H and ¹³C-NMR spectra of compound 7h.



8a



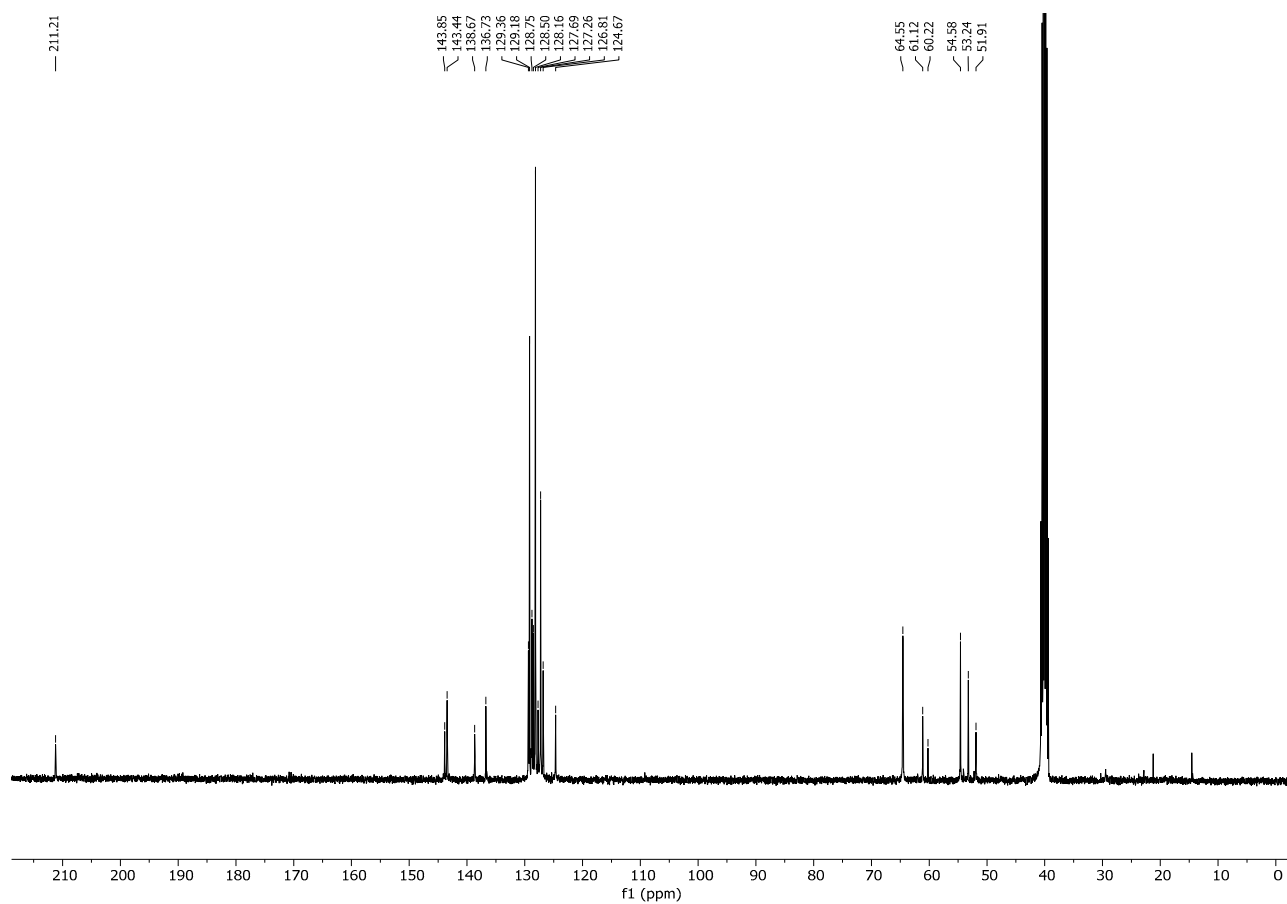
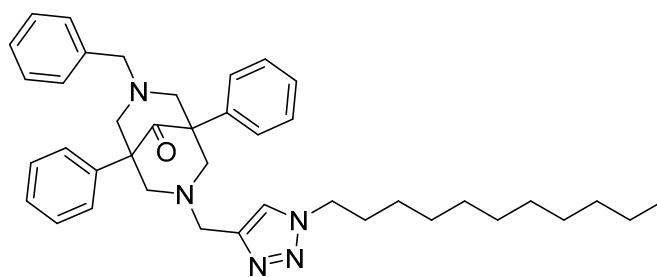
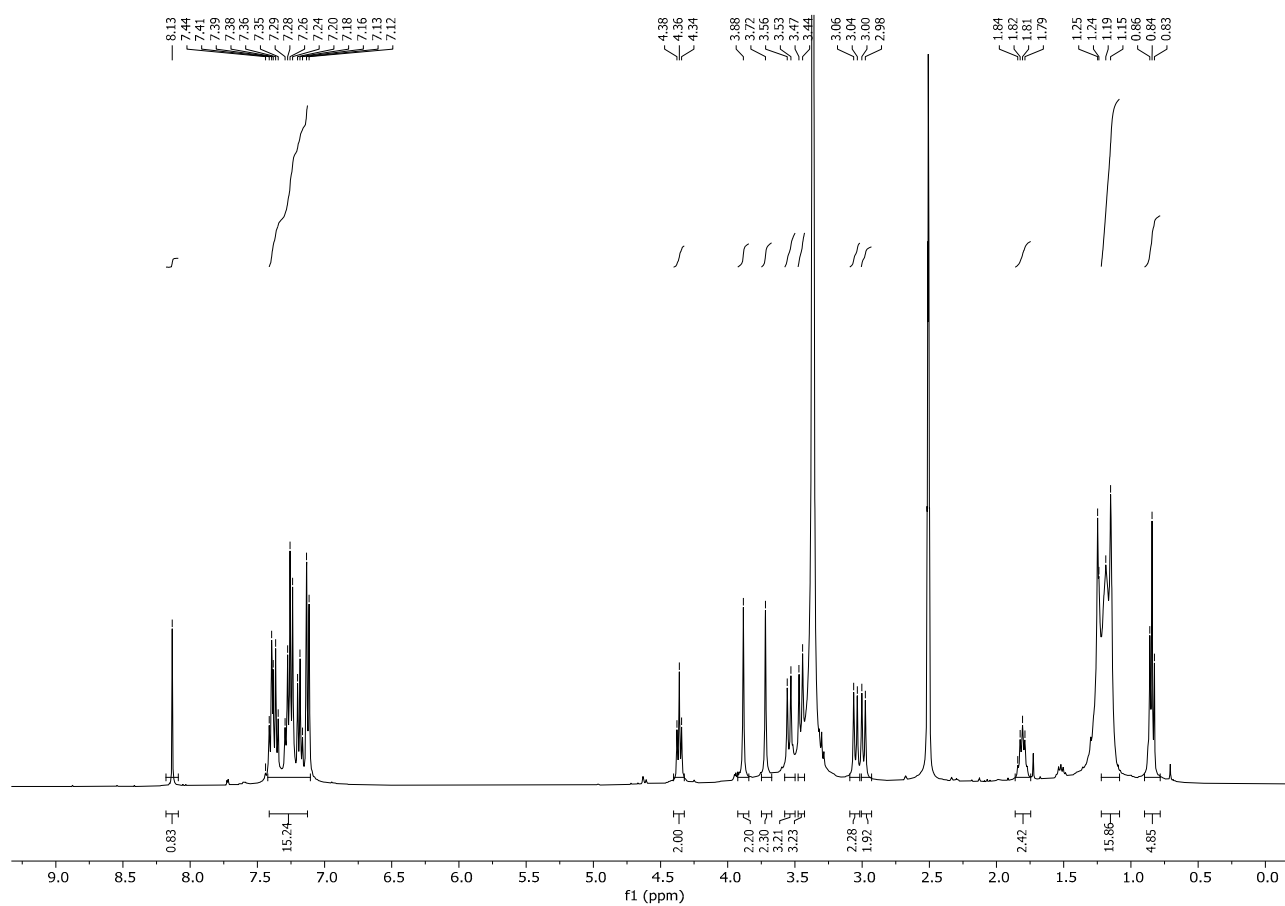


Figure S24. ^1H and ^{13}C -NMR spectra of compound 8a.



8b



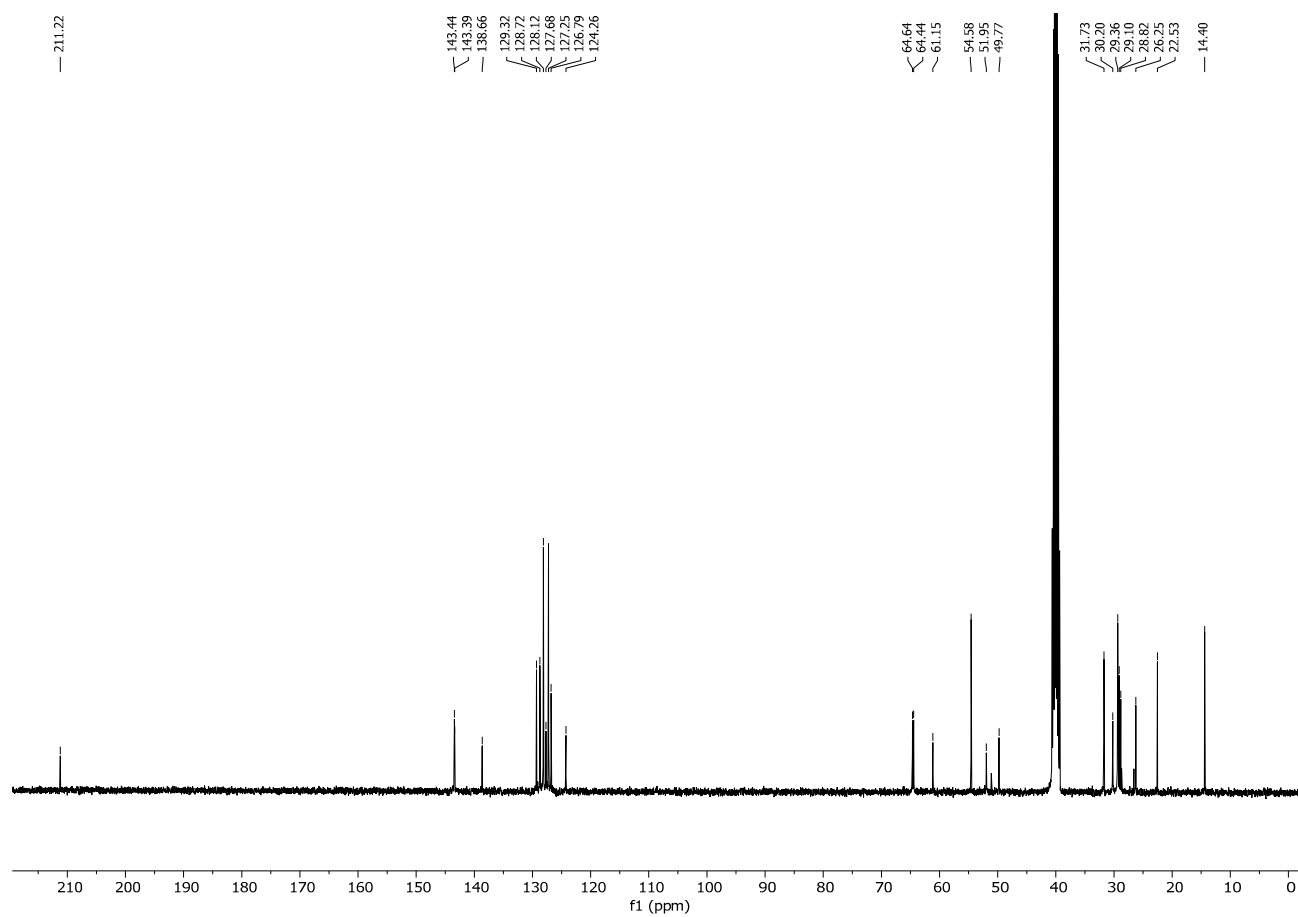
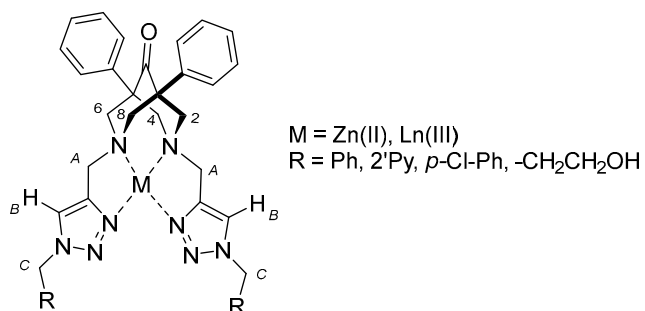


Figure S25. ^1H and ^{13}C -NMR spectra of compound **8b**.

2. NMR TITRATION OF BISPIDINE-METAL COMPLEXES

Table S1. Comparison of the free ligands **7a,b,d,h** and their metal complexes: list of the $\Delta\delta$ in the ^1H -NMR spectra.



Entry	Compound	$\Delta\delta$ for H _{2,4,6,8} eq (ppm)	$\Delta\delta$ for H _{2,4,6,8} ax (ppm)	$\Delta\delta$ for H _A (ppm)	$\Delta\delta$ for H _B (ppm)	$\Delta\delta$ for H _C (ppm)
1	7b ·Zn(II)	0.46	0.44	0.18	0.50	0.15
2	7d ·Zn(II)	0.50	0.61	0.27	0.24	0.15
3	7d ·La(III)	0.45	0.70	0.43	0.23	0.03
4	7a ·La(III)	0.46	0.71	0.42	0.24	0.04
5	7h ·La(III)	0.45	0.70	0.40	0.40	0.05

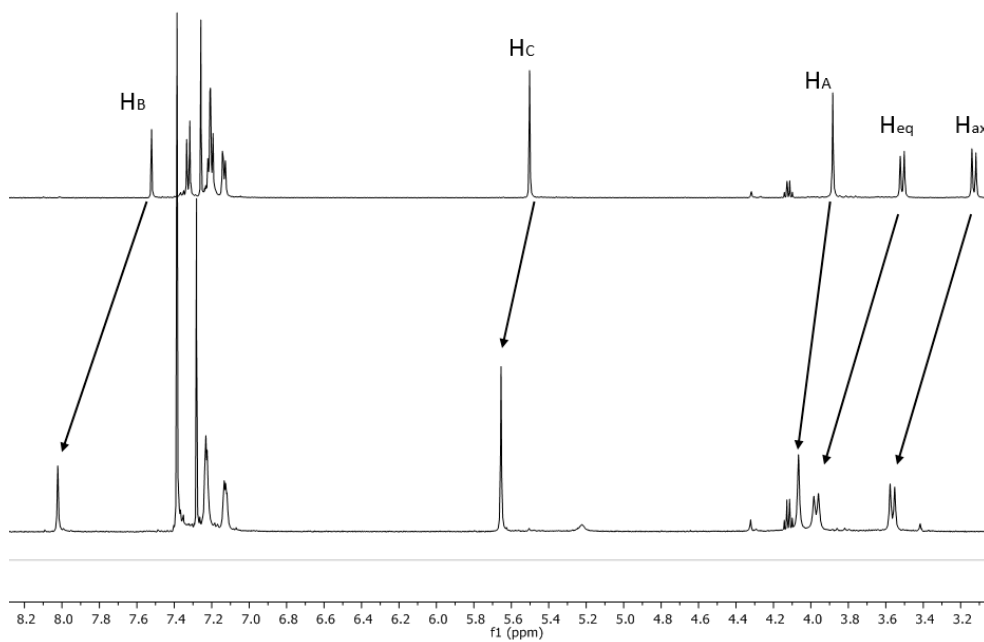


Figure S26. ^1H -NMR spectrum of compound **7b** and its Zn(II)-complex, **7b**·Zn(II).

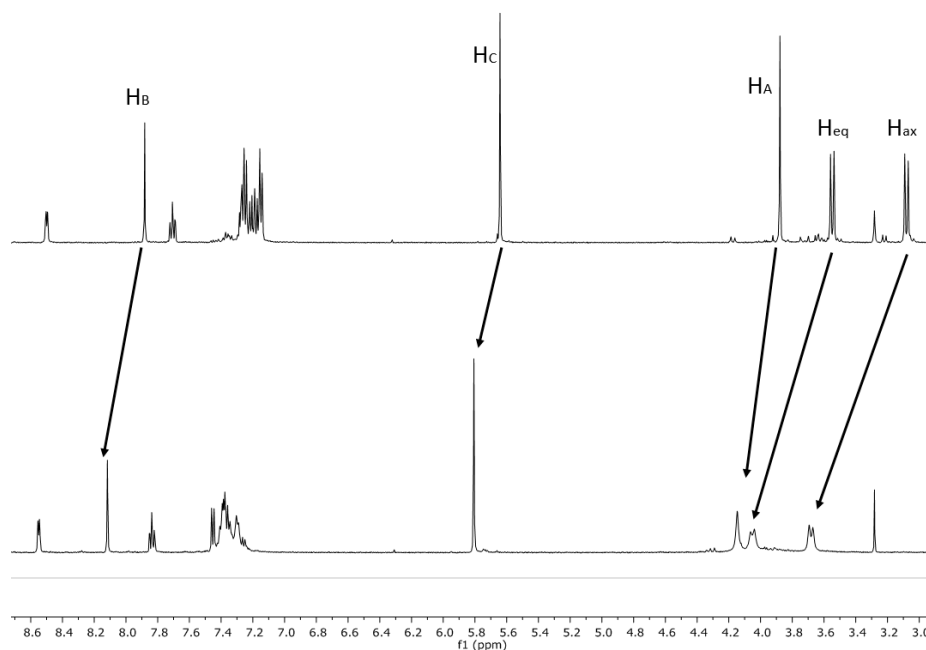


Figure S27. ¹H-NMR spectrum of compound **7d** and its Zn(II)-complex **7d-Zn(II)**.

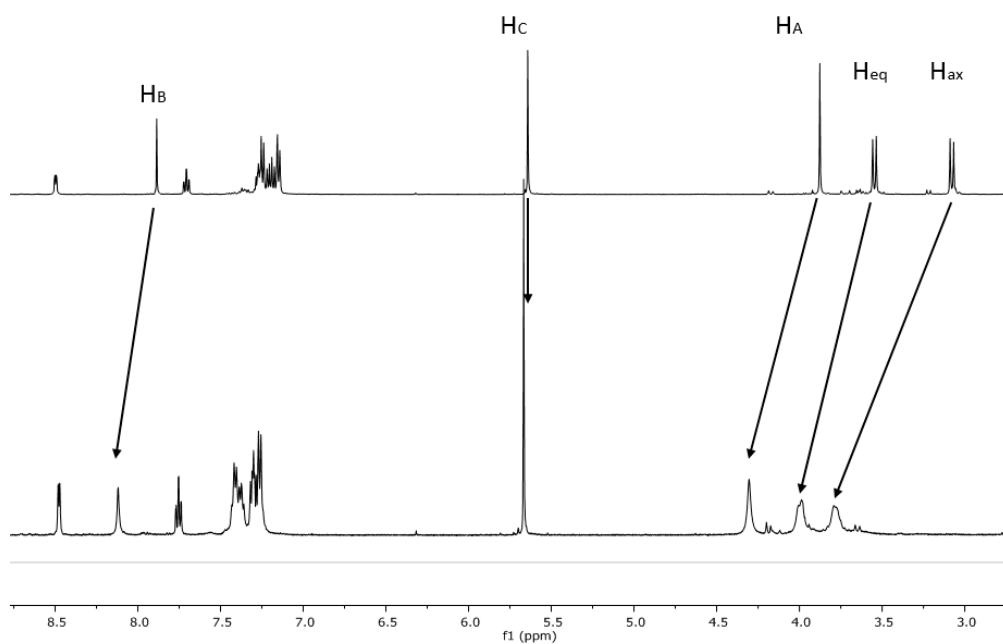


Figure S28. ¹H-NMR spectrum of compound **7d** and its La(III)-complex **7d-La(III)**.

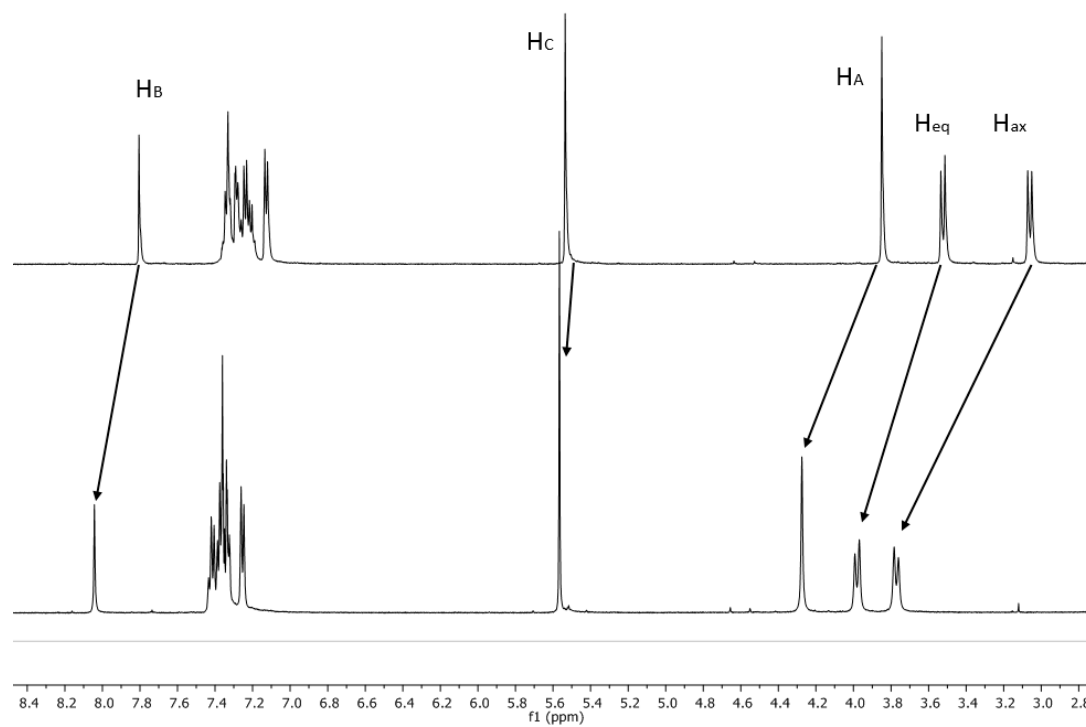


Figure S29. ¹H-NMR spectrum of compound **7a** and its La(III) complex **7a·La(III)**.

3. ESI-MS ANALYSIS

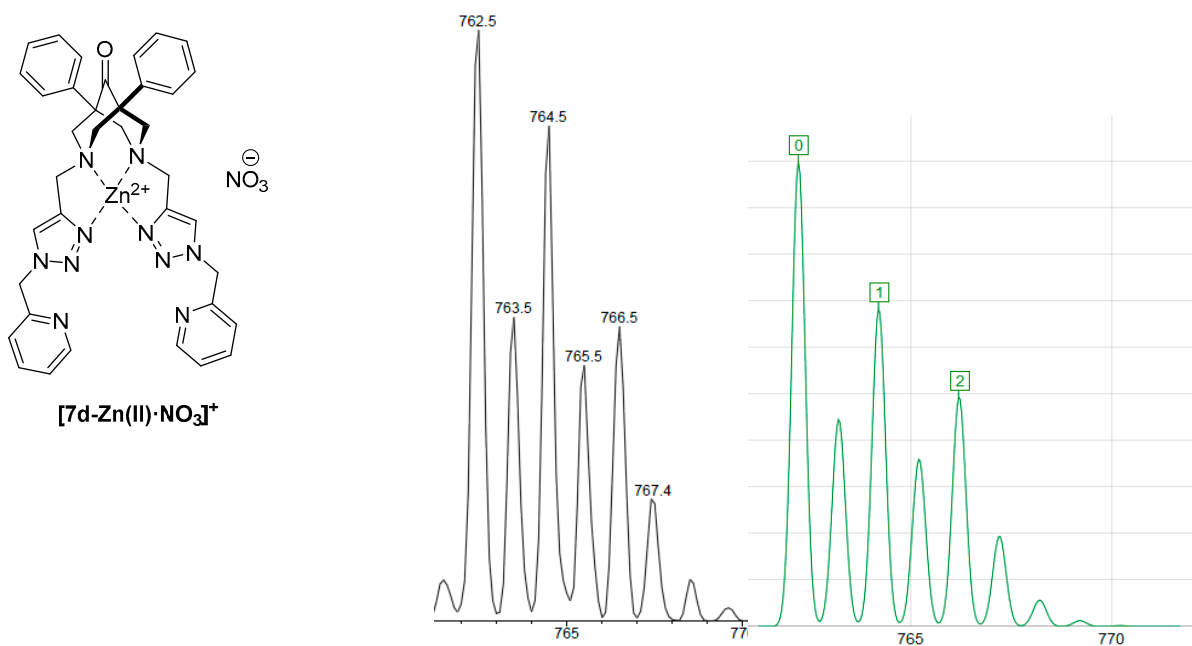


Figure S30. Comparison of the experimental ESI-MS spectrum of compound **[7d-Zn(II)·NO₃]⁺** (left) and the simulation of the isotopic pattern for the elemental composition $[C_{37}H_{36}N_{11}O_4Zn]^+$ (right).

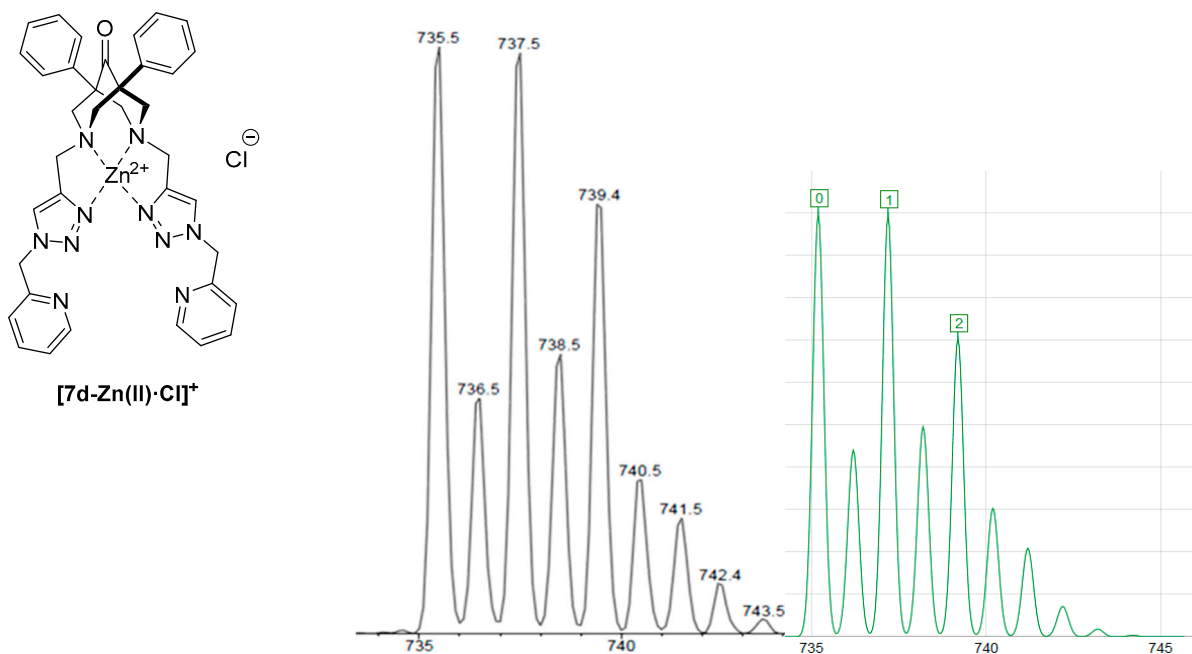


Figure S31. Comparison of the experimental ESI-MS spectrum of compound **[7d-Zn(II)·Cl]⁺** (left) and the simulation of the isotopic pattern for the elemental composition $[C_{37}H_{36}ClN_{10}OZn]^+$ (right).

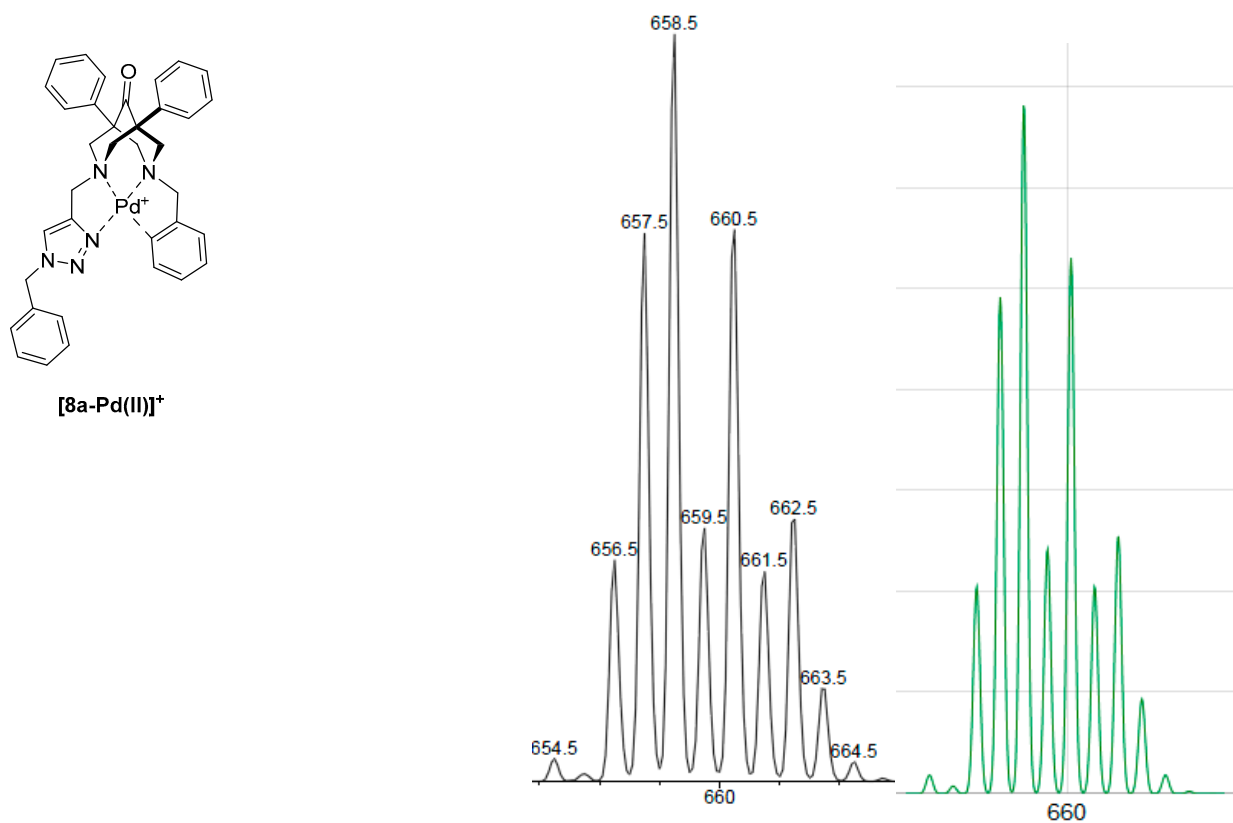


Figure S32. Comparison of the experimental ESI-MS spectrum of compound **[8a-Pd(II)]⁺** (left) and the simulation of the isotopic pattern for the elemental composition $[C_{36}H_{34}N_5OPd]^+$ (right).

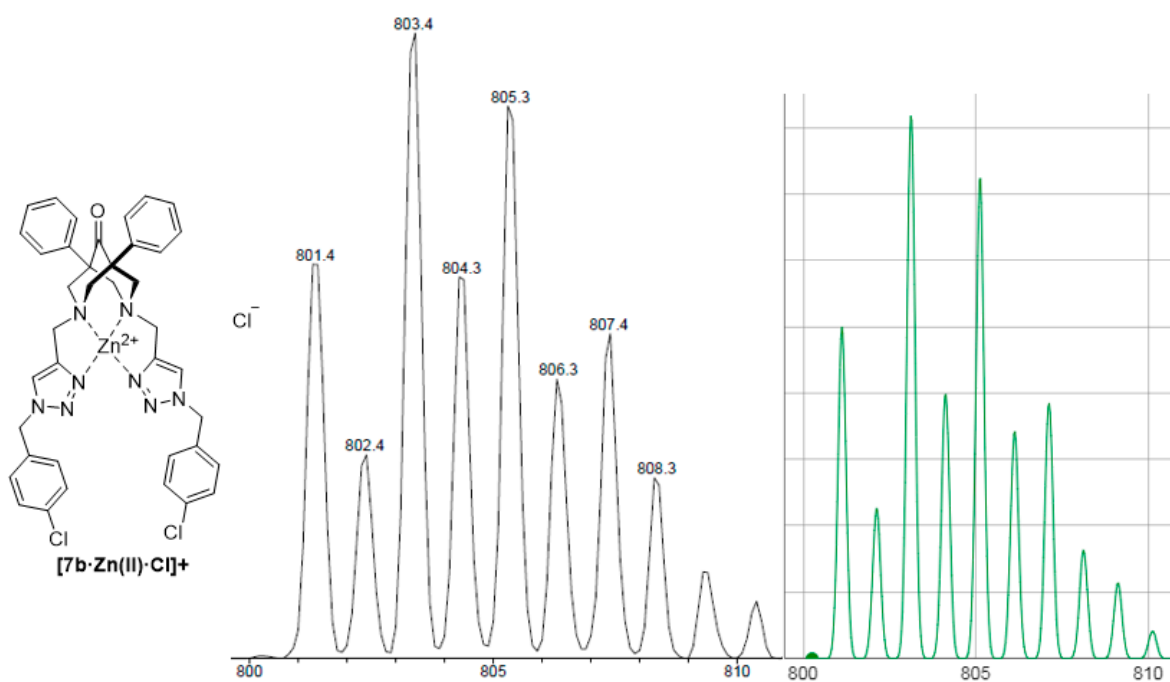


Figure S33. Comparison of the experimental ESI-MS spectrum of compound **[7b-Zn(II)·Cl]⁺** (left) and the simulation of the isotopic pattern for the elemental composition $[C_{39}H_{36}Cl_3N_8OZn]^+$ (right).